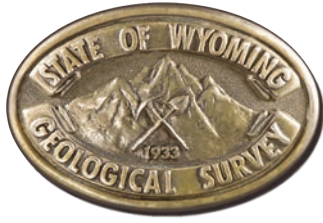


Interpreting the past, providing for the future

Preliminary Investigation of Quaternary Faults in Eastern Jackson Hole, Wyoming

By Seth J. Wittke

Open File Report 2017-1
March 2017



Wyoming State Geological Survey

Thomas A. Drean, Director and State Geologist



Preliminary Investigation of Quaternary Faults in Eastern Jackson Hole, Wyoming

By Seth J. Wittke

Layout by Christina D. George

Open File Report 2017-1
Wyoming State Geological Survey
Laramie, Wyoming: 2017

For more information on the WSGS, or to download a copy of this Open File Report, visit www.wsgs.wyo.gov or call 307-766-2286.

This Wyoming State Geological Survey (WSGS) Open File Report is preliminary and may require additional compilation and analysis. Additional data and review may be provided in subsequent years. The WSGS welcomes any comments and suggestions on this research. Please contact the WSGS at 307-766-2286, or email wsgs-info@wyo.gov.

Citation: Wittke, S.J., 2017, Preliminary investigation of Quaternary faults in eastern Jackson Hole, Wyoming: Wyoming State Geological Survey Open File Report 2017-1, 11 p.

Table of Contents

Abstract	1
Introduction	1
Previous Work	2
Geologic Setting	2
Methods	3
Antelope Flats	3
General Description	3
Geomorphology	4
Scarp Profiles	5
Summary	6
Faults South of Blacktail Butte.	6
General Description	6
Geomorphology	7
Scarp Profiles	7
Summary	8
Flat Creek Fan Faults.	8
General Description	8
Geomorphology	9
Scarp Profiles	9
Summary	10
Discussion and Conclusions.	10
Acknowledgments	11
References	12
Appendix	14

ABSTRACT

Jackson Hole valley contains numerous faults that are Quaternary age. The Teton fault is the most notable; however, numerous other faults can also be found in the valley. Three fault systems consisting of the faults at Antelope Flats, south of Blacktail Butte, and on the Flat Creek fan, are located along the eastern margin of the valley. The faults displace outwash and alluvial surfaces of Bull Lake (Munger Mountain) or younger age; however, they are not confirmed to be independently seismogenic. Light detecting and ranging (LiDAR) data, coupled with photogrammetric analysis of aerial photography, were used to refine prior mapping of the faults and map local geomorphic features. Elevation profiles across scarp sections were analyzed in order to calculate scarp offsets. In total, 36 profiles were extracted across the three fault systems. Scarp profile analysis shows scarp offsets across the Antelope Flats system to range from ~ 0 – 1.4 m. Net offsets at Blacktail Butte were relatively small (~ 0.5 m) compared to primary and antithetic offsets within the graben, and on the Flat Creek fan, scarp offsets ranged from ~ 0 – 1.7 m. Empirical regressions were used to calculate moment magnitudes associated with each fault system. In all three systems, moment magnitude (M_m), based on average and maximum scarp height, averaged $\sim M_m 6.6$. However, based on scarp rupture length, moment magnitudes were considerably less ($\sim M_m 5.5$). This study provides preliminary results based on topographic analysis of the faults. Future studies on specific fault systems are required to determine whether the faults are independently seismogenic or related to other tectonic sources in the area.

INTRODUCTION

The Jackson Hole valley is bound by the Teton Mountains to the west and the Gros Ventre Range to the east (fig. 1). Jackson Hole is a 71-km-long, asymmetric Tertiary structural basin in the hanging wall of the Holocene-active Teton fault. The Teton fault system on the eastern edge of the Teton Mountains has long been recognized as the most active fault system in the valley (White, 2006). However, the Jackson Hole valley also contains many other faults currently assigned ages ranging from Holocene to Late Quaternary (Machette and others, 2001a). The primary goal of this investigation is to evaluate a system of predominately westward-dipping late-Quaternary faults that form a distributed system of short, unconnected segments along the eastern edge of the valley.

In general, the fault systems on the east side of the Jackson Hole valley comprise a zone of north-south trending discontinuous, west-facing scarps. These distributed faults are described by two entries in the U.S. Geological Survey's (USGS) Quaternary Fault and Fold Database and are made up of both Class A and Class B faults. The USGS designates faults that have an undefined source or unconfirmed Quaternary activity as Class B. Seismogenic faults with recognized Quaternary offset are designated as Class A.

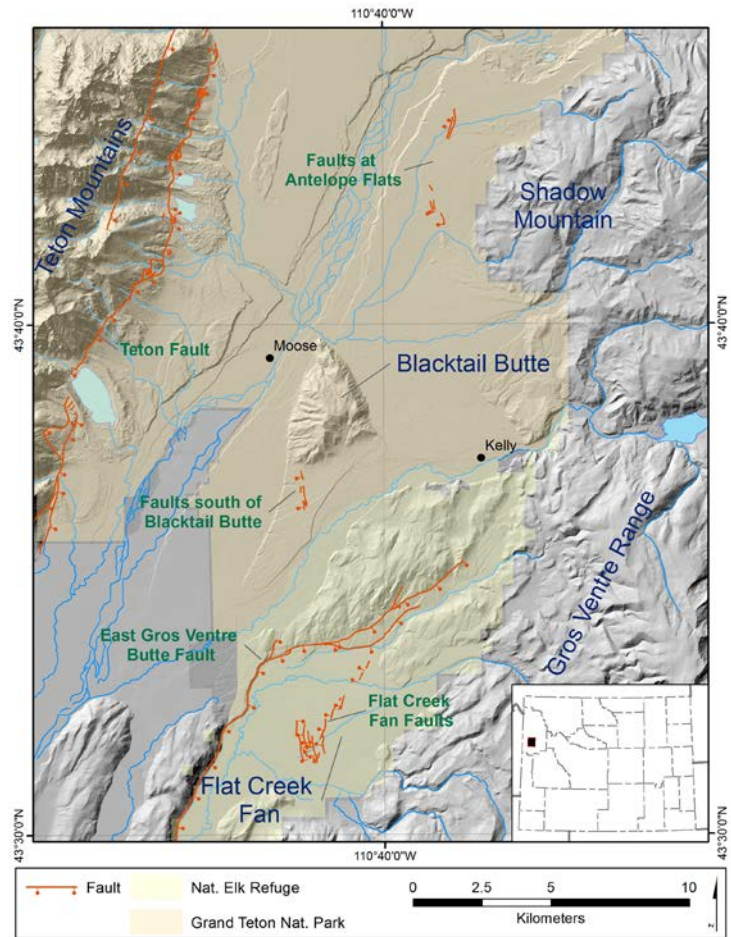


Figure 1. Map showing the Jackson Hole valley with relevant fault locations and features.

Secondary faults in Jackson Hole valley (USGS fault No. 725) include Class B faults that are generally antithetic to the Teton fault (Machette and others, 2001a). The secondary faults include those at the Potholes, north of the Snake River, at Antelope Flats, west of Shadow Mountain, and near Flat Creek, within the National Elk Refuge (fig. 1). Faults south of Blacktail Butte (USGS fault No. 724) are recognized by the USGS as Class A late-Quaternary faults (Pierce, 2001; fig. 1). Pierce notes that, similar to the Class B secondary faults (No. 725), the faults south of Blacktail Butte could also be secondary features related to a larger fault in the area. It is not clear why the faults south of Blacktail Butte are considered Class A faults while the other faults along the eastern Jackson Hole valley are designated as Class B.

This study focuses on the magnitude of vertical surface offsets and the geomorphic expression of fault scarps at Antelope Flats, south of Blacktail Butte, and on the Flat Creek fan (fig. 1). Recently acquired light detecting and ranging (LiDAR) data for the Grand Teton National Park (2014) along with the most recent aerial photographs that maintain stereo coverage in the area (U.S. Department of Agriculture, 2004) provide data ideal to revisit prior work regarding these features. In particular, scarp topographic profiles and surface age estimates from previous geologic mapping are used to bracket offset events.

PREVIOUS WORK

Gilbert and others (1983) studied the Jackson Hole valley faults as part of a seismotectonic study of the Jackson Lake Dam for the U.S. Bureau of Reclamation. They found that faults south of Blacktail Butte offset loess deposits about 0.6 m (net) along the main scarp (Gilbert and others, 1983). Gilbert and others also report that the faults on the Flat Creek fan show 0.6 m of net displacement over a 2.7 km length. Gilbert and others (1983) recognized that the faults are distributed over a wide (1–2 km) area, but suggest because of their small net offset and short scarp lengths, the faults may be related to strong ground motions associated with another fault in the area. Faults found in Antelope Flats are mentioned briefly in the Gilbert report but are not described in detail.

Geologic maps for the eastern portion of Jackson Hole include the Moose and Gros Ventre Junction quadrangle maps at 1:24,000 scale (Love 2001a, Love 2001b, respectively). The Moose quadrangle map does not show the faults at Antelope Flats. However, the Gros Ventre Junction quadrangle map does show the extent of the fault south of Blacktail Butte and generalized faults on the Flat Creek fan.

In 2000, Wong and others analyzed the seismic hazard for multiple dams in the area, including Island Park, Grassy Lake, and Jackson Lake dams. The report did not address the faults included in this report as they were considered too short to generate earthquakes (≤ 10 km).

GEOLOGIC SETTING

This region has undergone numerous episodes of deformation, including Sevier compression, Laramide uplift and compression, and Cenozoic Basin and Range extension. From the late-Tertiary to the present day, some of the Laramide and Sevier structural features have been overprinted or transected by north-south trending Tertiary, and in some cases Quaternary, high-angle normal faulting due to Basin and Range extension (Horberg and others, 1949). Cenozoic-aged normal faults coincide with north-northwest trending folds and thrust faults, which bound uplifts, creating range-front bounding faults that define a series of half-grabens. The Teton fault is the principal structure responsible for the Late Miocene to Holocene footwall uplift of the Teton Range and the hanging wall subsidence of the Jackson Hole basin (Smith and others, 1993).

The Neogene Teton Mountains (fig. 1) are superimposed over the northwest portion of the older Gros Ventre Range (Smith and others, 1993). The Teton Range is in the Intermountain Seismic Belt (ISB), which is a major

active seismic belt extending 1,300 km from Arizona through Utah, eastern Idaho, western Wyoming, and western Montana. The range is a tilted block of Precambrian basement rocks and overlying Paleozoic sedimentary strata, including significant deposits of limestone and dolomite. The range displays a vertical uplift of more than 7 km, inferred from the highest sedimentary rock to the depth of the basement of approximately 5 km underneath Jackson Hole (Smith and others, 1993).

The Gros Ventre Range bounds the eastern flank of Jackson Hole (fig. 1) and is a northwest trending Laramide uplift consisting of Precambrian basement rock underlying a generally continuous Paleozoic, Mesozoic, and Tertiary sedimentary section. The range is west of the Wind River Range and south of the Absaroka Mountains. It is bounded to the southwest by the northwest-striking Cache Creek thrust fault, which consists of a broad asymmetrical anticline with a steep and locally faulted southwest limb. The western portion of the Gros Ventre Range is transected by Tertiary faults. Older structures continue to the north across the Jackson Hole valley and into the Teton fault block. Several bedrock buttes containing Paleozoic rocks are exposed in the central and southern parts of the valley and are also exposed on the eastern flank of the Teton Range, west of the Teton fault.

The Quaternary geology in the valley consists of fluvial, alluvial, glacial, and volcanoclastic deposits, underlain by Tertiary fluvial, lacustrine, and volcanoclastic deposits (Smith and others, 1993). Glacial deposits in the valley floor are derived from two primary glacial advances into the valley. The Bull Lake equivalent (~150 ka) Munger Mountain glacial advance covered the valley floor with ice, leaving moraine deposits as far south as Hoback Junction, 20 miles south of the study area (Pierce and Good, 1992). The more limited Pinedale-aged glacial advance (~14 ka) left deposits at the mouths of valleys but did not extend far onto the valley floor. Terminal moraines associated with Pinedale glacial pulses impound water, creating many of the lakes found along the valley margins.

The Teton range front is a product of one of the most active normal faults in the ISB. The Teton fault, a 55-km-long system extending along the eastern base of the Teton Range, is a normal fault that originated as early as 5 million years ago and displays Holocene displacement (Smith and others, 1993). Late Quaternary fault scarps, ranging from 3 m to approximately 46 m high, are exposed along the entire extent of the Teton fault. The youngest fault scarps of the Teton fault offset post-Pinedale-age fluvial surfaces.

METHODS

A literature search was completed to compile existing geologic and map data for faults in the Jackson Hole valley. One m-pixel bare-earth LiDAR data and photogrammetry techniques were used to refine fault locations and identify additional scarps and lineaments. Field work was conducted in fall 2016 to photograph the mapped scarps/lineaments, measure profiles, and document local geomorphology. Field work resulted in refinement of fault locations, addition of previously unrecognized scarps, and removal of lineaments that did not appear to be faults after field checking.

Elevation profiles were extracted from the LiDAR data in ArcGIS and analyzed to calculate vertical-surface offset using a MatLab[®] script. Subsets of individual elevation profiles were selected in MatLab[®] to simplify calculations. For this reason, a specific scarp profile figure will show a different length than the profile shown in the fault maps (figs. 3, 6, and 8). Where grabens are present, primary and antithetic scarp offsets were calculated. For completeness, net scarp offset was also calculated across the entirety of individual grabens. To evaluate statistical uncertainties, at least three iterations for each scarp profile were calculated. Empirical regressions from Wells and Coppersmith (1994) were used to estimate magnitudes based on fault surface trace length and average and maximum single-event offsets. Scarp degradation models based on equations from Andrews and Buckman (1987) were considered, but only four scarp profiles met the model requirements (Scarp slope – Lower far-field slope > 10). For that reason, age estimates based on scarp degradation models were not included in this report.

ANTELOPE FLATS

General Description

The Antelope Flats fault system is made up of six discontinuous fault sections found west of Shadow Mountain and are considered to be in the hanging wall of the Teton fault. The faults trend north to south and extend about 9 km across deposits mapped as Munger Mountain (Bull Lake) glacial outwash at the western contact with relict glacial deposits of the same age (fig. 2). Scarp offset is primarily westward, although some sections are made up of grabens that also display eastward, antithetic displacement. The scarps display varying offsets within the glacial outwash terrains and a large alluvial fan. Although the faults offset Munger Mountain glacial deposits (~150 ka), they are considered Class B faults due to their having an undefined source (Machette and Pierce, 2001a). Gilbert and others (1983) suggest the faults could be secondary features related to either local unmapped subsurface faults or preferential settlement associated with a seismic event on the Teton fault.

Geomorphology

The Antelope Flats fault system consists of six separate scarp sections (fig. 3). The northernmost section is a readily recognizable graben roughly 20 m wide and 100 m long. South of the obvious graben that occupies the surface mapped as outwash 3, lineaments, interpreted as scarps, are present in a large alluvial fan, named the Shadow Mountain fan for the purpose of this report. The Shadow Mountain fan is interpreted to be a Late-Pleistocene feature comprised of early Pinedale-aged glacial material related to the Burned Ridge phase of the Pinedale glaciation sequence. The fan appears to cover the Munger Mountain surface (outwash 3) and has been reworked in places by (assumed) Holocene stream channels and fans, mapped as Holocene alluvium in figure 3. The three surfaces roughly bracket the Shadow Mountain fan between

the Munger Mountain outwash surface and Holocene alluvial deposits (~150–12 ka). Due to the episodic nature of alluvial fan development and the size of the fan, it is possible that it is made up of surfaces and deposits of varying ages within the Burned Ridge glacial episode.

The scarps within the Shadow Mountain fan are extremely subtle. Without the aid of LiDAR, it is likely they would not have been recognized with traditional methods. Since it is assumed that the fan is younger than surface 3, it suggests that the scarp sections were present when the fan was deposited on the outwash 3 surface, essentially obscuring the offset of the scarps. However, it is important to note the fault sections associated with profiles AF04–06 roughly parallel the general shape of the Shadow Mountain alluvial fan (fig. 3). The distribution of the fault sections on the fan surface, coupled with the small offsets, does not

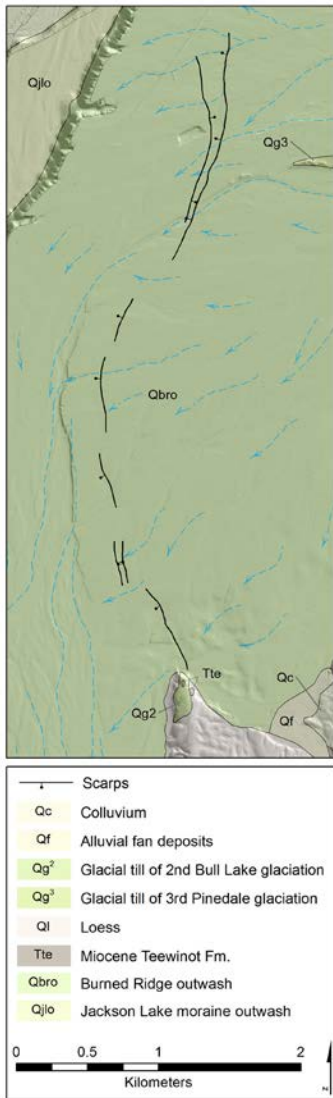


Figure 2. Antelope Flats area, showing mapped lineaments/scarps and local geology (Love, 2001).

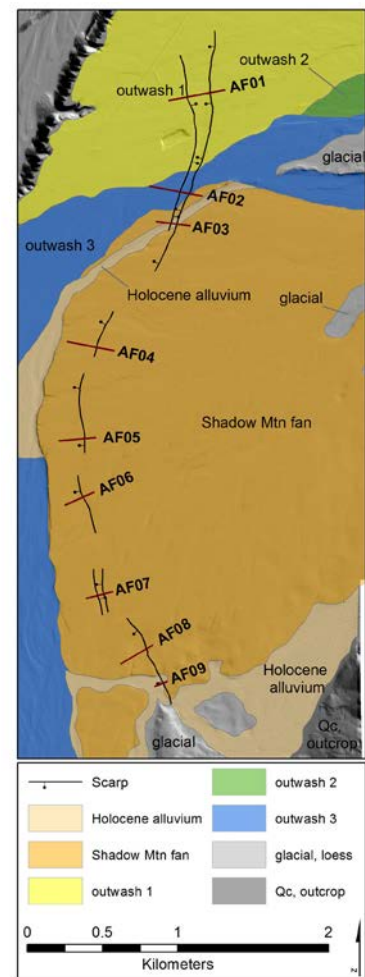


Figure 3. Geomorphic surfaces mapped in the Antelope Flats area. Three Bull Lake-aged outwash surfaces have been mapped, based on relative elevation. Map also shows Holocene alluvium dissecting the Burned Ridge alluvial fan.

preclude a non-tectonic cause for these sections. It is possible that the scarps are nothing more than lobes within the alluvial fan body.

The southern sections of the Antelope Flats fault sections begin to show increased offsets as they trend toward the southern extent of the Shadow Mountain fan. The fan thins to the south, which may provide less material to cover the scarp, suggesting the fan is post event. As the fault exits the fan, it enters glacial till and Holocene alluvial deposits (fig. 3), and as in outwash surface 3, forms a graben.

Scarp Profiles

Nine profiles were extracted from LiDAR data across the fault sections at Antelope Flats (fig. 3). Where grabens were present, primary and antithetic scarp offset was measured, as was net scarp offset (table 1). Profiles in the Antelope Flats area show scarp offsets <1.5 m, suggesting single event ruptures. Profile AF01 shows a scarp offset of 1.38 ± 0.13 m, while net offset at profile AF02 was calculated as 0.99 ± 0.12 m. The profiles show good upper and lower surface agreement and a well-defined scarp. AF03 was sampled across what is proposed as a Holocene alluvial surface that dissects the northern edge of the Munger Mountain fan (fig. 4). Although the surface appears offset using a hillshade dataset extracted from LiDAR, a profile extracted across the surface does not show a conclusive scarp in the Holocene surface.

Profiles AF04, AF05, and AF06 show consistent upper and lower far-field surfaces. The calculated scarp offset is much smaller than seen at profiles AF01 and AF02 (0.27 ± 0.03 , 0.06 ± 0.02 , and 0.08 ± 0.04 m, respectively). The small offsets on the Shadow Mountain fan are hard to distinguish from the variability of the surrounding ground surface. This suggests that the mapped scarp sections are potentially non-tectonic and related to alluvial lobes within the fan itself. Although, as previously mentioned, the fan may obscure the true offset of scarp sections. Scarp profiles not shown in the report can be found in the appendix.

Profile AF07 shows a small graben with a net offset of 0.58 ± 0.06 m. The net offset agrees well with the difference between the primary (1.32 ± 0.16 m) and antithetic (0.72 ± 0.06 m) calculations. Profiles AF08 and AF09 were extracted from a section located on the lateral portion of a fan where deposits become dominated by glacial till and Holocene alluvial deposits. The hummocky surface related to the glacial till along profile

Table 1. Characteristics derived from elevation profile analysis for scarps in the Antelope Flats area. So (Scarp offset) is shown in meters, Ls (Lower far-field slope), Us (Upper far-field slope), and Ss (Scarp slope) are shown in degrees. Negative slopes represent westward facing surfaces while positive values are eastward facing. All values are from horizontal. P=Primary, A=Antithetic, and N=Net.

Profile	So (m)	Ls (Deg)	Us (Deg)	Ss (Deg)
AF01	1.38 ± 0.13	-0.63 ± 0.11	-1.48 ± 0.28	-8.74 ± 0.63
AF02-P	1.16 ± 0.08	-0.63 ± 0.19	-1.38 ± 0.06	-7.22 ± 1.18
AF02-A	0.25 ± 0.03	-0.19 ± 0.10	-0.26 ± 0.02	1.97 ± 0.01
AF02-N	0.99 ± 0.12	-0.33 ± 0.09	-1.53 ± 0.05	-4.36 ± 0.64
AF03	NA	NA	NA	NA
AF04	0.27 ± 0.03	-1.08 ± 0.06	-1.66 ± 0.00	-1.66 ± 0.79
AF05	0.06 ± 0.02	-1.3 ± 0.07	-1.31 ± 0.04	-2.54 ± 1.05
AF06	0.08 ± 0.04	-2.31 ± 0.38	-1.77 ± 0.08	-1.89 ± 0.53
AF07-P	1.32 ± 0.16	-1.08 ± 0.40	-1.56 ± 0.35	-13.37 ± 0.44
AF07-A	0.72 ± 0.06	0.45 ± 0.04	-0.32 ± 0.17	3.63 ± 0.17
AF07-N	0.58 ± 0.06	-0.43 ± 0.08	-1.36 ± 0.32	-13.35 ± 0.44
AF08-P	0.6 ± 0.02	-0.88 ± 0.05	-1.9 ± 0.16	-8.81 ± 0.40
AF08-A	0.28 ± 0.01	-0.02 ± 0.11	-0.81 ± 0.11	1.32 ± 0.12
AF08-N	-0.01 ± 0.11	-0.73 ± 0.04	-1.91 ± 0.11	-9.37 ± 0.68
AF09-N	0.22 ± 0.08	-0.38 ± 0.14	-1.16 ± 0.02	-4.61 ± 0.05

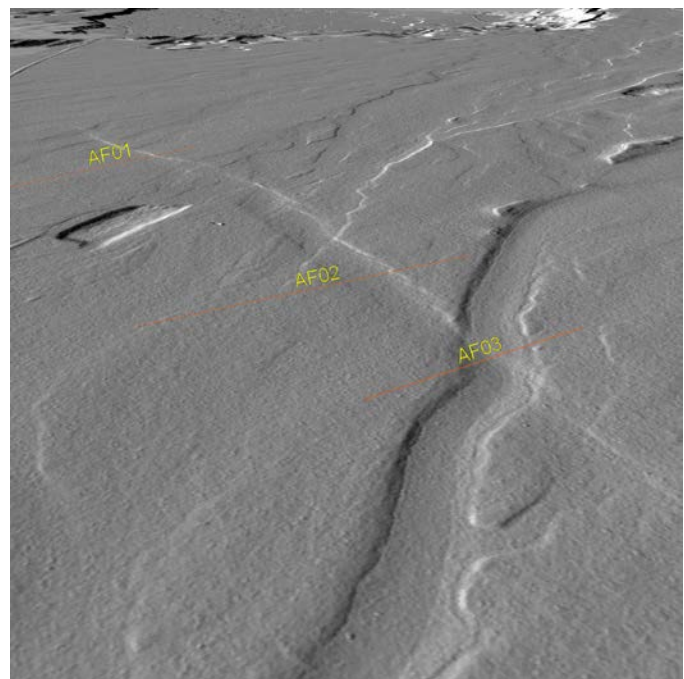


Figure 4. Oblique view of hillshade showing northern graben at Antelope Flats. Profile AF03 appears to cross a small offset within a drainage that dissects the Burned Ridge fan.

AF08 likely complicated the scarp offset calculation. The primary scarp offset is calculated as 0.6 ± 0.02 m, while the antithetic scarp offset is 0.28 ± 0.01 m. Comparison of the AF08 primary and antithetic faults show a net offset across AF08 of 0.32 ± 0.01 m, which differs than the calculated -0.01 ± 0.11 m net scarp offset (table 1). The graben at AF09 is poorly formed and may be, in part, obscured by alluvium. A primary and antithetic scarp was not recognizable along the profile. For that reason, only a net scarp offset of 0.22 ± 0.08 m was calculated.

Using empirical regressions from Wells and Coppersmith (1994) based on fault rupture surface trace length as well as average and maximum single-event offsets, moment magnitudes were calculated for the fault sections at Antelope Flats (table 2). For this calculation, the fault sections are considered coeval, single-event scarps. Although the average and maximum scarp offsets provide reasonable results for surface rupturing seismic events, 6.55 ± 0.05 and 6.71 ± 0.03 m, respectively, the overall rupture length of the scarps calculate to a magnitude 5.83 ± 0.01 m.

Summary

Profiles calculated across fault sections in the Antelope Flats area provided scarp offsets ranging from 1.38 ± 0.13 m in the northern Antelope Flats area to 0.06 ± 0.02 m within the Shadow Mountain fan. The scarp offsets are greatest in the northern and southern extents of the area, although offsets in the north are almost twice the offsets observed in the south. The scarp sections within the Shadow Mountain fan show very small offsets, nearly indistinguishable from the natural variance of the ground surface. It remains unclear whether these sections are tectonic or merely lobes within the alluvial fan itself.

The relatively short fault sections compared to the calculated offset suggests a complex zone of deformation at Antelope Flats. Based on Wells and Coppersmith (1994), the overall rupture length does not equate to an independent seismic source large enough to cause surface deformation. However, the average and maximum displacement regressions do provide magnitudes large enough to form scarps.

FAULTS SOUTH OF BLACKTAIL BUTTE

General Description

Similar to the faults at Antelope Flats, the faults south of Blacktail Butte occupy the hanging wall of the Teton fault. The west-dipping fault system is characterized by an 80-m-wide graben that extends roughly 1.5 km across offset outwash surfaces covered with loess (fig. 5). The surfaces are mapped by Love (2001b) as coeval with the second Bull Lake major glaciation and derived from glacial outwash from the Gros Ventre River drainage. The surfaces are mantled by loess up to 3 m in depth (Pierce, 2001). Pierce notes the outwash surfaces are likely of early-Pinedale age, not Bull Lake as mapped by Love. Love (2001b) mapped multiple Quaternary-aged normal faults south of Blacktail Butte. However, the mapped faults may actually be terrace facies associated with the glacial outwash surfaces. This alternate

Table 2. Results from Wells and Coppersmith's (1994) empirical regressions calculating moment magnitude from surface rupture length, average scarp offset, and maximum scarp offset in the Antelope Flats area.

		Mm
Surface rupture length (km)	4.5 ± 0.1	5.83 ± 0.01
Average displacement (m)	$0.44 \pm .07$	6.55 ± 0.05
Maximum displacement (m)	1.38 ± 0.13	$6.71 \pm .03$

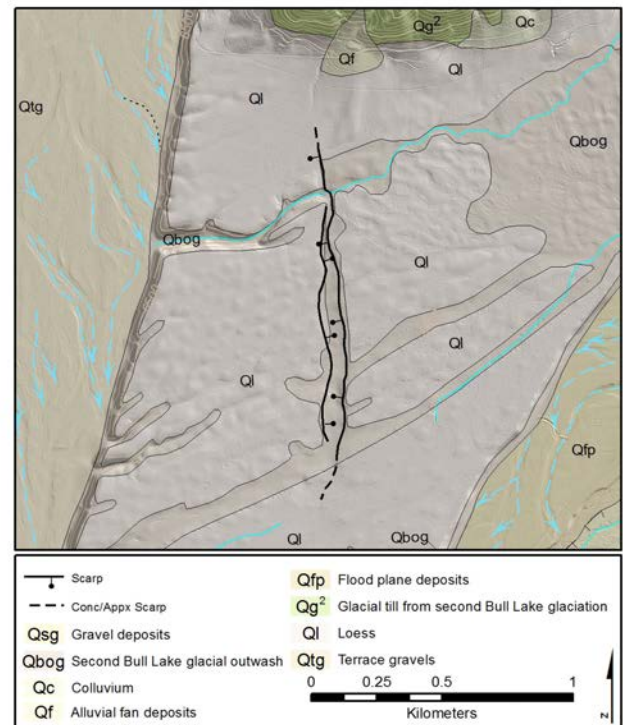


Figure 5. Geologic map of the area south of Blacktail Butte. Bull Lake-aged outwash (Qbog) and loess (Ql) are offset by a graben formed by the faults south of Blacktail Butte (Love, 2001b).

interpretation is corroborated by the fact that only one of the normal faults mapped by Love is included in the USGS Quaternary Faults and Folds Database even though they are shown to offset Quaternary units.

Geomorphology

The faults south of Blacktail Butte form a graben that offsets two distinct outwash surfaces (fig. 6). Outwash Surface 1 is the lowest and presumably the youngest of the three outwash surfaces. Surface 2 is approximately 3 m above Surface 1, while Surface 3 is 10 m higher in elevation than Surface 2. The faults do not appear to offset Surface 3, however, a lineament does extend from the scarp to the south a short distance into the older surface. Loess has infilled portions of the graben and surrounding outwash surfaces. Although this provides a late age bracket for the graben (-12 ka), it also obscures portions of the fault, potentially affecting the fault scarp calculations.

The northern portion of the fault is obscured by an alluvial fan that postdates Surface 1 (fig. 6). Love (2001b) mapped the fault extent northward into the fan and bedrock, however, a topographic profile calculated across the feature suggests the feature is more likely a gully related to a small debris flow originating from the flank of Blacktail Butte. The fault may extend to the north under the fan, however, it is not exposed at the surface.

Scarp Profiles

Table 3 shows the scarp offsets measured at four profiles across the graben, including the west-facing primary scarp and east-facing antithetic scarp. The faulted surfaces are hummocky, making scarp profiles difficult to interpret. Scarp profiles not shown in the report can be found in the appendix. Profile BB01 shows an offset along the primary scarp of 1.72 ± 0.36 m and an antithetic scarp offset of 1.62 ± 0.08 m. The scarp offsets are very similar, and with the calculated uncertainties are essentially identical.

Table 3. Characteristics derived from elevation profile analysis for scarps in the area south of Blacktail Butte. So (Scarp offset) is shown in meters, Ls (Lower far-field slope), Us (Upper far-field slope), and Ss (Scarp slope) are shown in degrees. Negative slopes represent westward facing surfaces while positive values are eastward facing. All values are from horizontal. P=Primary, A=Antithetic, and N=Net.

Profile	So (m)	Ls (Deg)	Us (Deg)	Ss (Deg)
BB01-P	1.72 ± 0.36	-1.81 ± 0.70	-0.52 ± 0.00	-11.76 ± 1.24
BB01-A	1.62 ± 0.08	-1.11 ± 0.47	-1.25 ± 0.11	3.06 ± 0.09
BB01-N	0.38 ± 0.17	-1.19 ± 0.13	-0.58 ± 0.06	-10.93 ± 1.88
BB02-P	2.78 ± 0.10	-0.84 ± 0.14	-2.16 ± 0.31	-6.21 ± 0.14
BB02-A	1.68 ± 0.13	-0.64 ± 0.18	-0.66 ± 0.02	2.20 ± 0.20
BB02-N	2.15 ± 0.25	-0.64 ± 0.08	-0.58 ± 0.04	-6.03 ± 0.38
BB03-P	4.12 ± 0.42	-1.67 ± 0.57	-2.08 ± 0.56	-12.38 ± 0.06
BB03-A	1.13 ± 0.18	0.51 ± 0.60	1.25 ± 0.13	9.68 ± 1.31
BB03-N	0.67 ± 0.38	-0.7 ± 0.12	-0.86 ± 0.09	-12.34 ± 0.06
BB04	NA	NA	NA	NA

A net offset of 0.38 ± 0.17 m was calculated from the scarp profile, which, although still small, more closely matches the 0.64 m of net offset calculated by Gilbert and others (1983). Inconsistent upper and lower far-field surfaces at BB02 (fig. 7) likely over estimate the net offset (2.15 ± 0.25 m). Profile BB03 shows a mean net offset of 0.67 ± 0.38 m; however, a comparison of the primary and antithetic faults at BB03 shows a calculated offset of 2.5 m to 3.0 m.

Visual analysis of a hillshade dataset extracted from the LiDAR data suggests the fault does extend for a short distance into outwash Surface 3. Love (2001b) also maps the scarp a short distance into Surface 3. Profile BB04 was calculated across the area where the scarp was inferred to be. However, the profile revealed no discernible offset (fig. 8). For this reason, the scarp is not believed to offset outwash Surface 3 south of Blacktail Butte, or if it does, the scarp

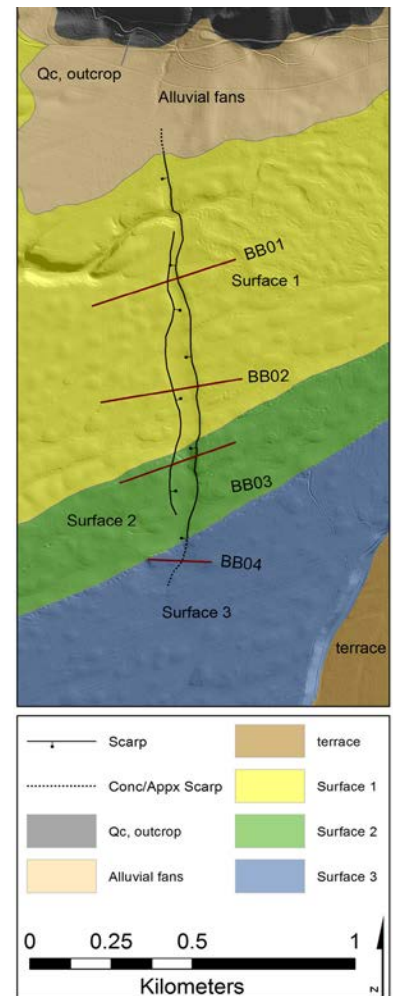


Figure 6. Geomorphic surfaces mapped south of Blacktail Butte. Three Bull Lake-aged surfaces have been mapped based on relative elevation.

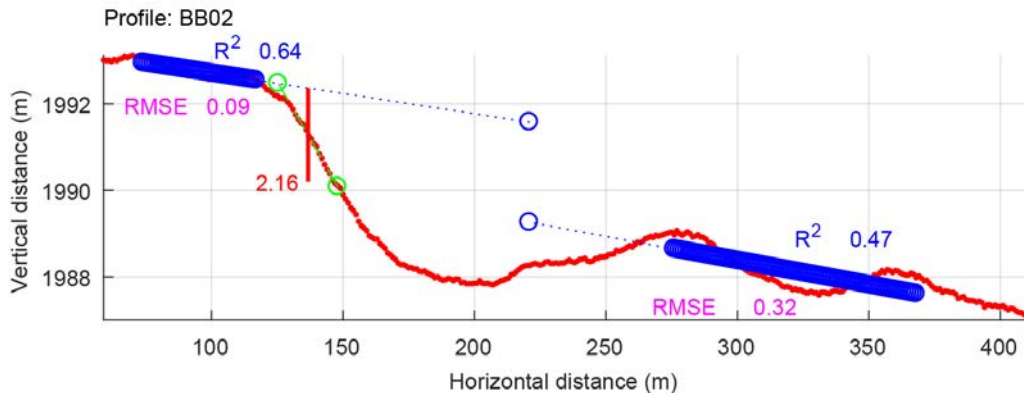


Figure 7. Scarp profile BB02 shown in graphical form. Profile is shown from east to west.

offset is small enough not to be discernible from the hummocky ground surface.

Wells and Coppersmith's (1994) regressions based on fault rupture surface trace length as well as average and maximum single-event offsets show moment magnitudes similar to those calculated at Antelope Flats (table 4). The resultant moment magnitudes are not consistent and raise questions about the relationship of the scarp offsets to the fault section length. Similar to the faults at Antelope Flats, the maximum and average offset regressions provide moment magnitudes sufficient for surface rupture (~Mm 6.7). However, moment magnitude based on surface rupture length is 5.25 ± 0.07 m, too small to displace the ground surface.

Summary

The hummocky outwash surfaces and loess cover make it difficult to calculate consistent scarp offsets. The uncertainties of the scarp characteristics are higher in the faults south of Blacktail Butte than at Antelope Flats or the Flat Creek fan. The appendix contains examples of the extracted profiles across the faults. Profiles show the irregularity of the surfaces and the difficulties encountered trying to calculate scarp offsets from them. Although the uncertainties are high, profiles BB01 and BB03 do confirm a small net offset across the faults as noted by Gilbert and others (1983). The faults show large enough displacements to be independently sourced. However, the short surface rupture lengths do not correlate to sufficient magnitudes. A Holocene-aged fan covers the northern extent of the faults; therefore, the actual surface rupture length may be longer. However, it is doubtful that the unmapped portion of the fault is long enough to greatly alter the result.

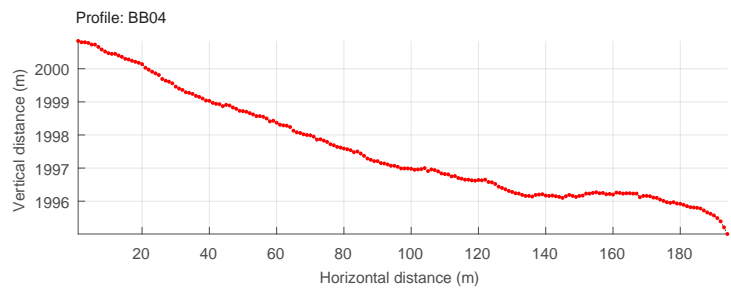


Figure 8. Scarp profile BB04 shown in graphical form. Profile is shown from east to west.

Table 4. Results from Wells and Coppersmith's (1994) empirical regressions calculating moment magnitude from surface rupture length, average scarp offset, and maximum scarp offset for the faults south of Blacktail Butte.

		Mm
Surface rupture length (km)	1.4 ± 0.2	5.25 ± 0.07
Average displacement (m)	0.74 ± 0.12	6.70 ± 0.05
Maximum displacement (m)	1.1 ± 0.14	6.64 ± 0.04

FLAT CREEK FAN FAULTS

General Description

In southeastern Jackson Hole, scarps offset a large early-Holocene alluvial fan sourced from the Flat Creek drainage, referred to by Gilbert and others (1983) as the Flat Creek fan. The scarps form a broad graben that is roughly 0.5 km wide to the south. To the north, the graben widens and separates into a single primary scarp with no apparent

antithetic fault. The scarps within the fault system are made up of westward-facing primary fault scarps with a few eastward-dipping antithetics (fig. 9). The Flat Creek fan is not related to localized glaciation, but rather Holocene-aged alluvial processes associated with streams, primarily Flat Creek flowing from the Gros Ventre Mountains (Love and Love, 1988). Flat Creek has entrenched itself in the northern part of the fan and is considered a perennial stream within the fan. There are also a few smaller perennial flows in other portions of the fan.

The Flat Creek fan system is east of the East Gros Ventre fault, a Class B fault as mapped by Love and Love (1988). Whereas the faults at Antelope Flats and south of Blacktail Butte are likely antithetic to the Teton fault, the faults on Flat Creek fan are potentially antithetic to the East Gros Ventre Butte fault. The East Gros Ventre fault is considered a Class B fault due to having an unknown source (Machette and Pierce, 2001b). It is unclear whether the fault is tectonic or the result of Pinedale-aged fluvial processes. This presents two distinct unresolved fault geometries. The faults could be antithetic to the Gros Ventre fault or the Teton fault.

Geomorphology

Scarps in the Flat Creek fan form a large, wide graben that narrows to the south (fig. 9). The graben is 3 km long and ranges from roughly 2 km wide in the north to 0.5 km wide in the south. The scarps that make up the graben are discontinuous, en echelon sections. Individual scarps within the graben show subtle offsets that vary in height and offset direction. Offsets suggest single-event scarps, however, it is unclear whether they are synchronous. The graben-bounding scarps are distinct; the eastern graben-bounding scarps dip west and are considered the primary scarp, while the western graben-bounding scarps, which dip east, are antithetic. Perennial streams and drainages on the fan have re-established themselves across the scarps.

Scarp Profiles

Table 5 shows the calculated vertical surface offsets for scarp profiles across the Flat Creek fan faults (fig. 9). Profiles ER01 and ER02 have similar offsets, 1.69 ± 0.25 and 1.34 ± 0.11 m, respectively. Scarps farther south, within the main graben, decrease in size but still show offsets greater than 0.5 m. Scarp profiles BB07 and BB08 sample the graben-bounding antithetic fault. Scarp offsets are 1.5 ± 0.02 m (ER07) and 1.39 ± 0.17 m (ER08). Profiles ER09 and ER10 are located on central graben scarps that show offsets that are effectively identical, although in opposite directions. Profile ER11 crosses a small scarp that, although visible in the hillshade, is indistinguishable in profile (fig. 10). For that reason, scarp offset calculations were not completed at profile ER11. Profile ER12 was extracted across the entirety of the graben to calculate the net offset of the system. Based on the model, net offset is 1.52 ± 0.13 m in the southern portion of

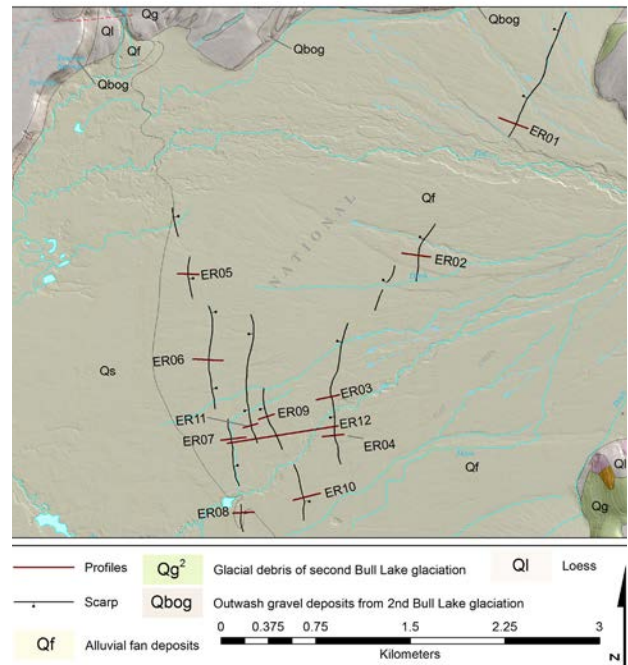


Figure 9. Geologic map of the Flat Creek fan fault system.

Table 5. Characteristics derived from elevation profile analysis for scarps in the Flat Creek fan area. So (Scarp offset) is shown in meters, Ls (Lower far-field slope), Us (Upper far-field slope), and Ss (Scarp slope) are shown in degrees. Negative slopes represent westward facing surfaces, while positive values are eastward facing. All values are from horizontal.

Profile	So (m)	Ls (Deg)	Us (Deg)	Ss (Deg)
ER01	1.69 ± 0.25	-1.32 ± 0.60	-1.66 ± 0.02	-6.82 ± 0.26
ER02	1.34 ± 0.11	-0.87 ± 0.18	-1.41 ± 0.16	-6.91 ± 2.37
ER03	0.71 ± 0.03	-1.39 ± 0.09	-1.66 ± 0.03	-6.91 ± 2.37
ER04	0.99 ± 0.13	-0.67 ± 0.15	-1.35 ± 0.35	-6.6 ± 0.61
ER05	0.51 ± 0.01	0.81 ± 0.03	0.75 ± 0.03	-0.67 ± 0.13
ER06	0.7 ± 0.01	0.6 ± 0.07	0.75 ± 0.02	-1.84 ± 0.43
ER07	1.5 ± 0.02	0.77 ± 0.07	0.43 ± 0.11	-10.9 ± 2.4
ER08	1.39 ± 0.17	0.88 ± 0.05	-0.01 ± 0.41	-6.62 ± 0.68
ER09	0.67 ± 0.01	-0.79 ± 0.01	-1.09 ± 0.02	1.841
ER10	0.66 ± 0.11	1.31 ± 0.19	0.72 ± 0.03	-2.64 ± 0.01
ER11	NA	NA	NA	NA
ER12	1.52 ± 0.13	-0.76 ± 0.00	-0.88 ± 0.09	-8.06 ± 0.15

the graben. The calculated net offset differs from a comparison of offsets calculated at ER04 and ER 07, which provides a net offset of roughly 0.5 m. Scarp profiles not shown in the report can be found in the appendix.

Moment magnitude calculations based on surface rupture length as well as average and maximum scarp offsets again provide dissimilar results (table 6). Average and maximum offsets provide moment magnitudes of roughly 6.8, while the short surface rupture length (4.1 km) results in a moment magnitude of 5.79.

Summary

The Flat Creek fan faults are dissimilar to the faults south of Blacktail Butte and at Antelope Flats in two ways. First, the fault system forms a wide graben structure instead of a single, narrow graben-forming scarp segment. Second, the fault system is potentially antithetic to the East Gros Ventre fault instead of the Teton fault. The fault also offsets younger surfaces than the faults to the north.

Faults on the Flat Creek fan display a graben structure made up of multiple en echelon sections that widen to the north. Scarp offsets in the fault system range from ~1.5 to 0.5 m, typical of single-event displacement. However, synchronicity between the fault sections has not been determined. Based on Wells and Coppersmith (1994), average and maximum scarp offsets provide large enough moment magnitudes for surface rupture, but as with the other faults in this study, the surface rupture length yields lower moment magnitude results.

DISCUSSION AND CONCLUSIONS

Faults at Antelope Flats and south of Blacktail Butte are considered to be in the hanging wall of the Teton fault. Scarps at Antelope Flats displace Bull-Lake-equivalent (~150 ka) outwash surfaces and may be covered, or partially obscured, by an early-Pinedale-aged alluvial fan. The faults south of Blacktail Butte displace surfaces that are believed to be late-Pleistocene to early Holocene. At Flat Creek, faulting postdates a fan surface that is possibly late Pleistocene to early Holocene in age (~14 ka). The Flat Creek fan faults are potentially in the hanging wall of the East Gros Ventre fault instead of the Teton fault.

The USGS considers the secondary faults in eastern Jackson Hole, including Antelope Flats and Flat Creek, to be Class B faults due to having an unknown source. Whether the faults south of Blacktail Butte are seismogenic is also in question. The faults show scarp offsets that are consistent with other small ISB faults, ranging from small (0.5 m) to moderate (1.5 m). Regressions based on Wells and Coppersmith (1994) show moment magnitudes calculated from scarp offset of roughly 6.75 for all fault systems. However, the rupture length for each fault system is shorter than typical seismogenic faults within the ISB.

This study was not able to confirm or deny whether the secondary faults in Jackson Hole, including faults south of Blacktail Butte, are independently seismogenic or related to other tectonic sources in the area.

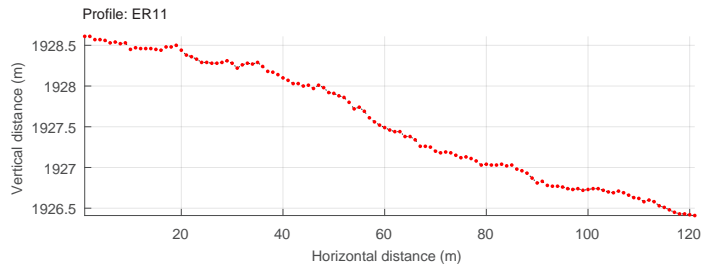


Figure 10. Scarp profile ER11 in graphical form. Profile is shown from west to east.

Table 6. Results from Wells and Coppersmith’s (1994) empirical regressions calculating moment magnitude from surface rupture length, average scarp offset, and maximum scarp offset in the Flat Creek area.

	Mm	
Surface rupture length (km)	4.14 ± 0.5	5.80 ± 0.06
Average displacement (m)	1.06 ± 0.09	6.80 ± 0.02
Maximum displacement (m)	1.69 ± 0.25	6.77 ± 0.05

The faults on the eastern side of Jackson Hole are distinct enough that further investigations should study specific faults rather than the group as a whole. Paleoseismic investigations, dating of offset surfaces, and geophysical analysis to better define subsurface fault geometry would all provide valuable information about the secondary faults in the valley.

DuRoss and Hylland (2015) investigated the intra-basin Wasatch fault zone and the relationship to the range-bounding Salt Lake City fault segment in Utah. In part, they found that large events on the Wasatch fault zone were typically synchronous with, or triggered by, events on the larger, or master, Salt Lake City segment. The report may prove to be relevant to the fault systems in this study if the faults are indeed antithetic to a larger seismogenic fault. In the case of the faults at Antelope Flats or south of Black-tail Butte, a segment of the Teton fault could prove to be the master fault. The faults on the Flat Creek fan could be antithetic to the East Gros Ventre Butte fault or the Teton fault further west.

There is currently insufficient data on these faults to perform an investigation similar to the Wasatch fault zone report. However, as future studies better define these faults, a detailed study comparing paleoseismic data to known events on the Teton fault or other seismic sources in the area would shed light on whether these features are related to ground motions from external events or are independently seismogenic. Focused studies will also validate whether a number of the lineaments are fault scarps or are related to other geomorphic features. As new information becomes available about these faults, the Class B designation by the USGS can be re-evaluated and updated as necessary.

ACKNOWLEDGMENTS

This project was funded through a cooperative agreement between the Wyoming State Geological Survey and the U.S. Geological Survey (Earthquake Hazards Program External Research Support Award # G16AP00008). Thank you to the USGS and staff, namely Richard Briggs, Christopher DuRoss, and Ryan Gold, for their review and help with this project. Christopher DuRoss provided the MatLab[®] script that was instrumental in the completion of the scarp analyses. Also, a thank you to Mort Larsen formerly of WSGS, for his help in initiating this project.

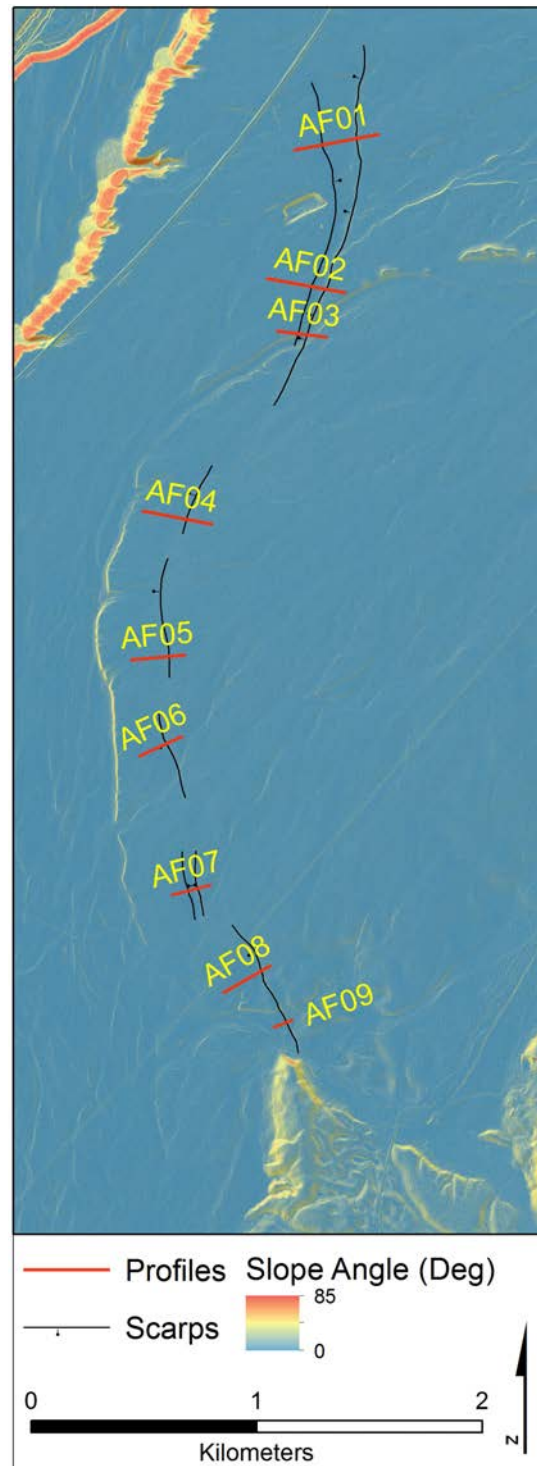
REFERENCES

- Andrews, D.J., and Bucknam, R.C., 1987, Fitting degradation of shoreline scarps by a nonlinear diffusion model, *Journal of Geophysical Research*, v. 92, issue B12, p. 12,857–12,867.
- DuRoss, C.B., and Hylland, M.D., 2015, Synchronous ruptures along a major graben-forming fault system: Wasatch and West Valley fault zones, Utah: *Bulletin of the Seismological Society of America*, v. 105, no. 1, p. 14–37.
- Gilbert, J.D., Ostenna, D., and Wood, C., 1983, Seismotectonic study of Jackson Dam and Reservoir, Minidoka Project, Idaho-Wyoming: U.S. Bureau of Reclamation Seismotectonic Report 83-8, 123 p., 11 pls.
- Horberg, L., Nelson, V., and Church, V., 1949, Structural trends in Central Western Wyoming: *Bulletin of the Geological Society of America*, v. 60, pp. 183-216.
- Love, J.D., and Love, J.M., 1988, Geologic road log part of the Gros Ventre River Valley including the Lower Gros Ventre slide: Wyoming Geological Survey [Wyoming State Geological Survey] Reprint 46, 14 p.
- Love, J.D., 2001a, Geologic map of the Moose quadrangle, Teton County, Wyoming: Wyoming State Geological Survey Love Map Series 3, scale 1:24,000.
- Love, J.D., 2001b, Geologic map of the Gros Ventre Junction quadrangle, Teton County, Wyoming: Wyoming State Geological Survey Love Map Series 3, scale 1:24,000.
- Machette, M.N., and Pierce, K.L., compilers, 2001a, Fault number 725, Secondary faults in Jackson Hole valley, in Quaternary fault and fold database of the United States: U.S. Geological Survey website, accessed December 2016, at <https://earthquakes.usgs.gov/hazards/qfaults>.
- Machette, M.N., and Pierce, K.L., compilers, 2001b, Fault number 756, East Gros Ventre fault, in Quaternary fault and fold database of the United States: U.S. Geological Survey website, accessed December 2016, at <https://earthquakes.usgs.gov/hazards/qfaults>. Pierce, K.L., compiler, 2001, Fault number 724, Faults south of Blacktail Butte, in Quaternary fault and fold database of the United States: U.S. Geological Survey website, accessed December 2016, at <https://earthquakes.usgs.gov/hazards/qfaults>.
- Pierce, K.L., and Good, J.D., 1992, Field guide to the Quaternary geology of Jackson Hole, Wyoming: U.S. Geological Survey Open File Report 92–504.
- Smith, R.B., Byrd, J.O.D., and Susong, D.D., 1993, The Teton fault, Wyoming—Seismotectonics, Quaternary history, and earthquake hazards, in Snoke, A.W., Steidtmann, J.R., and Roberts, S.M., eds., *Geology of Wyoming: Wyoming Geological Survey of Wyoming* [Wyoming State Geological Survey] Memoir 5, p. 628–667.
- Wells D.L., and Coppersmith K.J., 1994, New empirical relationships among magnitude, rupture length, rupture width, rupture area, and surface displacement, *Bulletin of the Seismological Society of America*, v. 84, n. 4., p. 974–1,002.
- White, B.J.P., 2006, Seismicity, seismotectonics, and preliminary earthquake hazard analysis of the Teton Region, Wyoming: Salt Lake City, University of Utah, M.S. thesis.
- Wong, I., Olig, S., and Dober, M., 2000, Preliminary probabilistic seismic hazard analyses-Island Park, Grassy Lake, Jackson Lake, Palisades, and Ririe Dams: U.S. Department of Interior, Bureau of Reclamation Technical Memorandum D8330-2000-17.

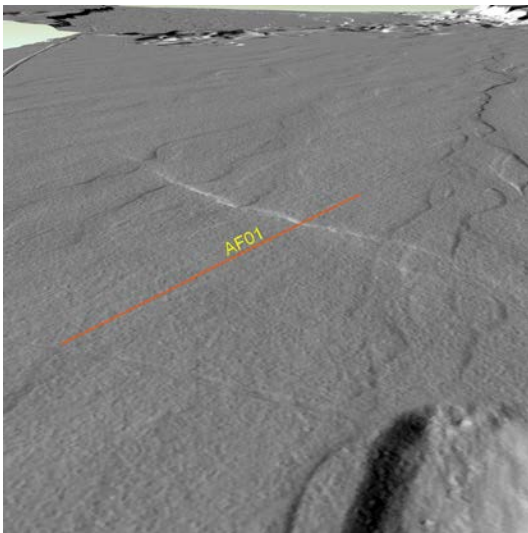
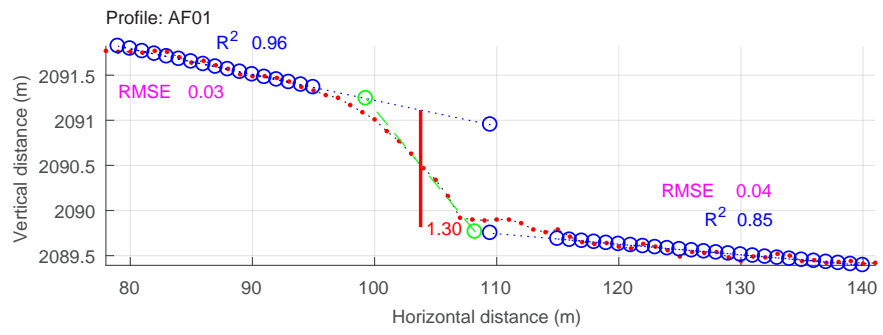
Appendix

The appendix includes all scarp profiles extracted from LiDAR along the three fault systems (Antelope Flats, south of Blacktail Butte, and at Flat Creek fan). The profiles shown are the author's preferred scarp profiles. Values shown in the appendix are different than the mean values presents in the report.

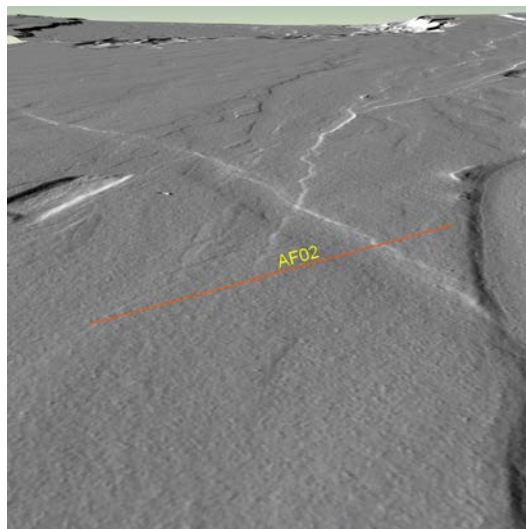
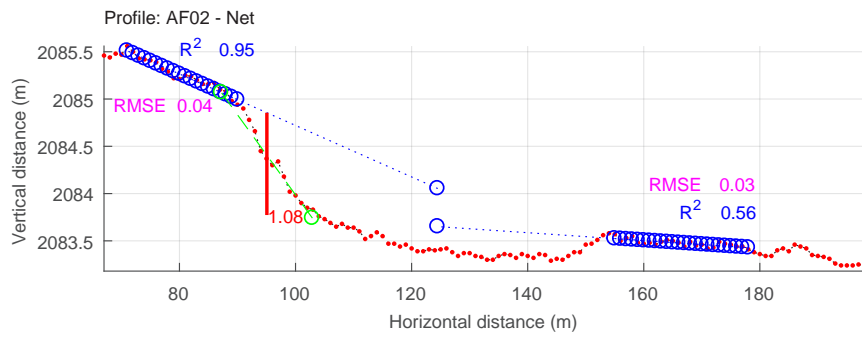
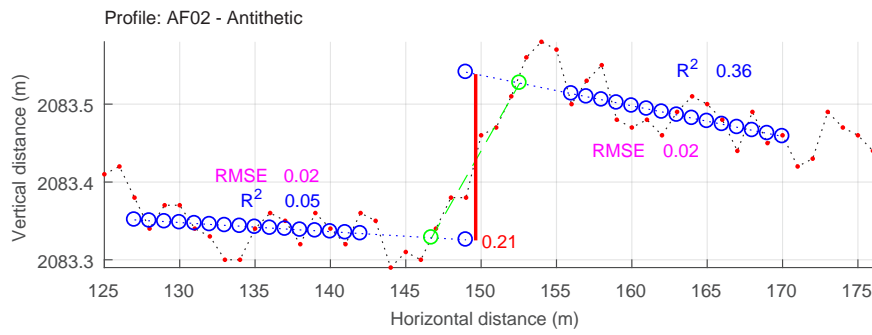
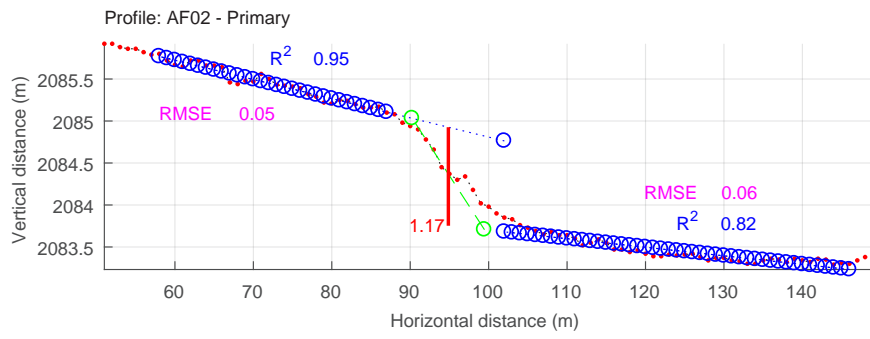
Map showing profile locations at Antelope Flats.



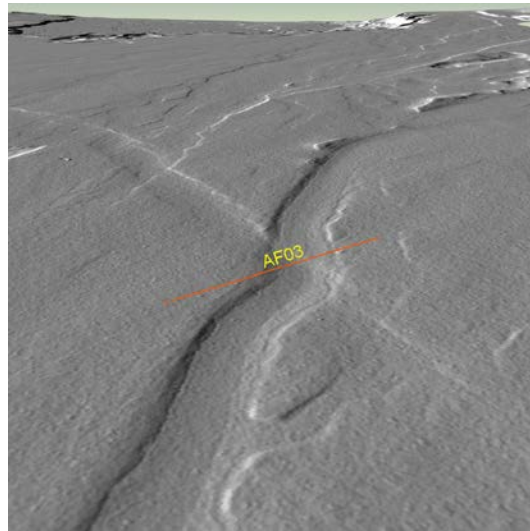
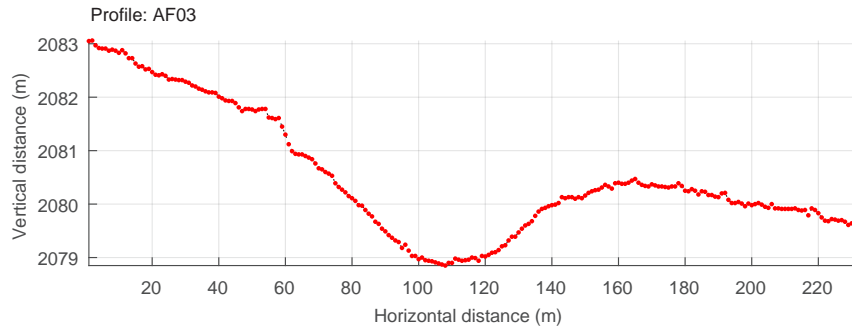
Elevation plot of AF01, including map of profile location and associate scarp and photograph.



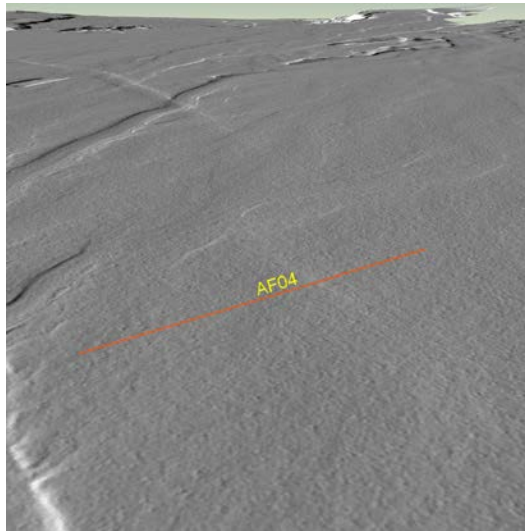
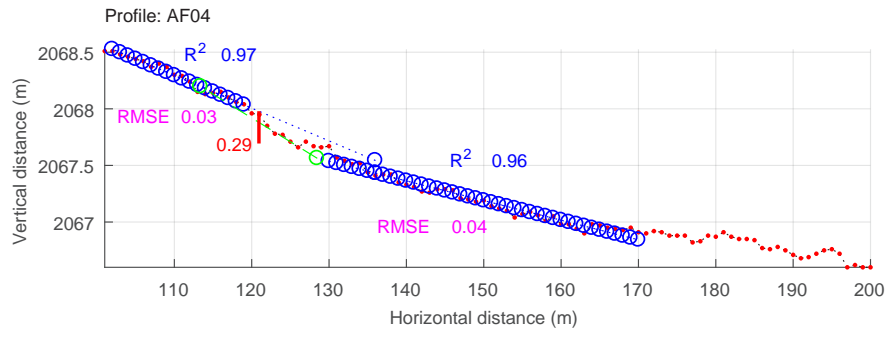
Elevation plots of AF02, including map of profile location and associate scarp.



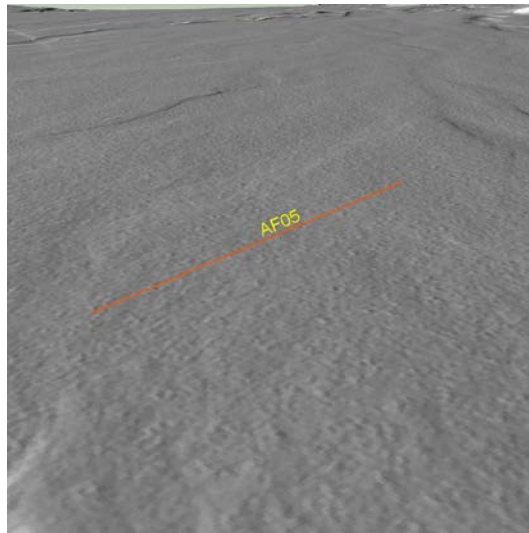
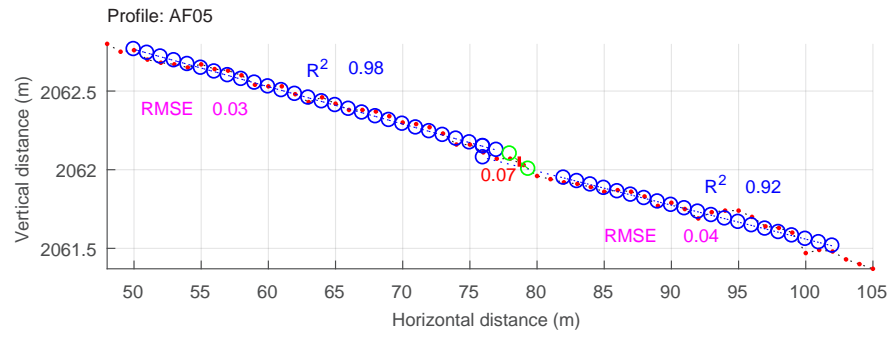
Elevation plot of AF03, including map of profile locations and associate scarp.



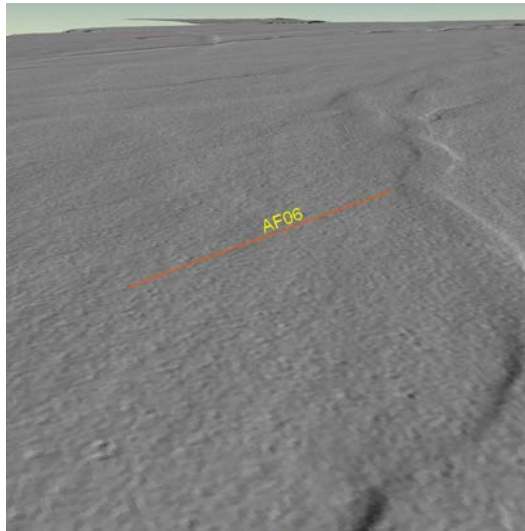
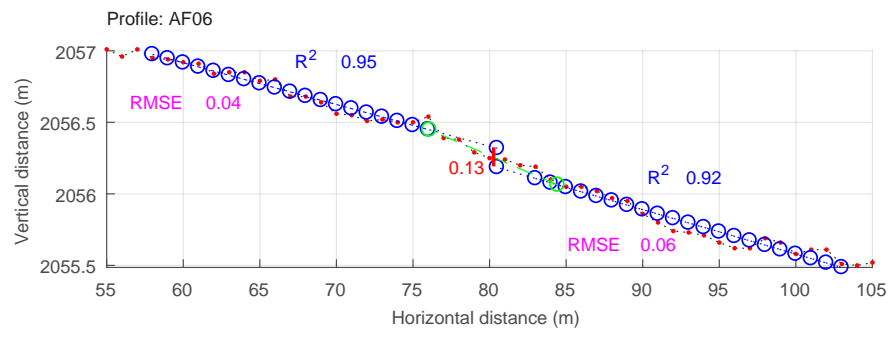
Elevation plot of AF04, including map of profile location and associate scarp.



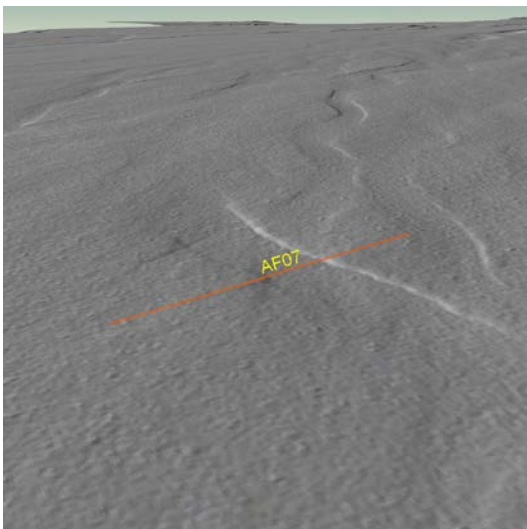
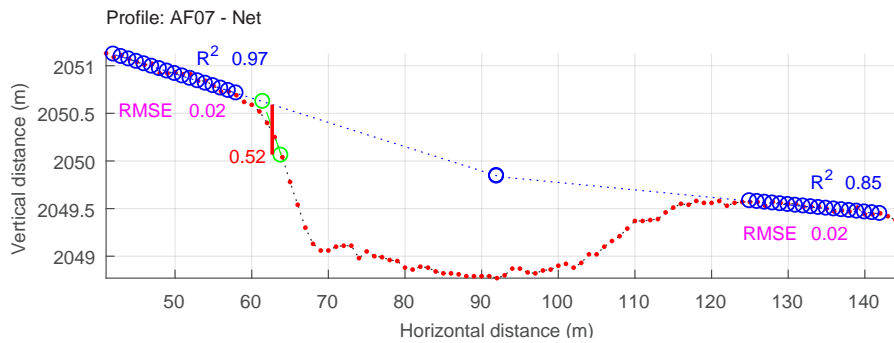
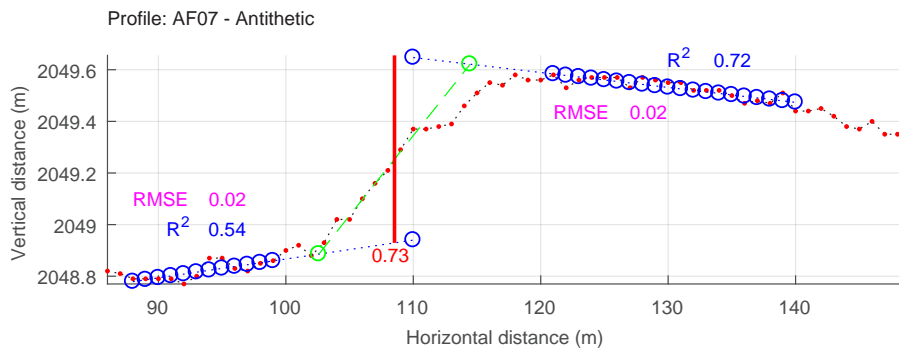
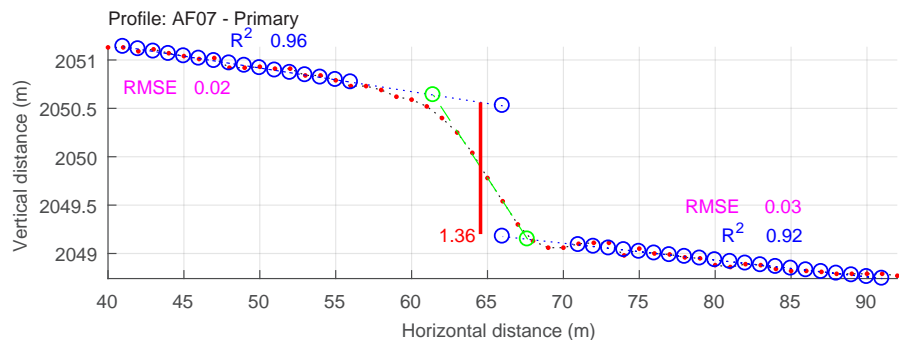
Elevation plot of AF05, including map of profile location and associate scarp.



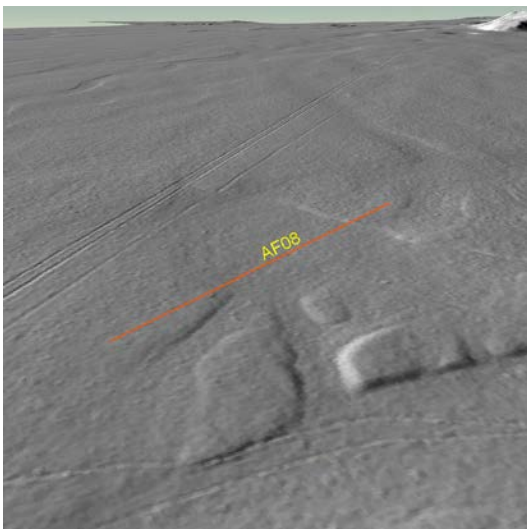
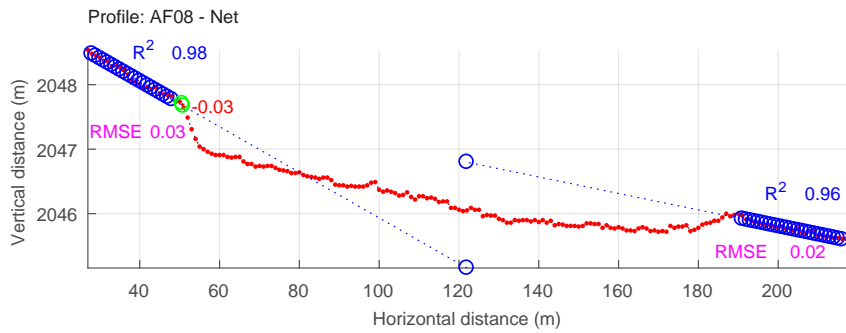
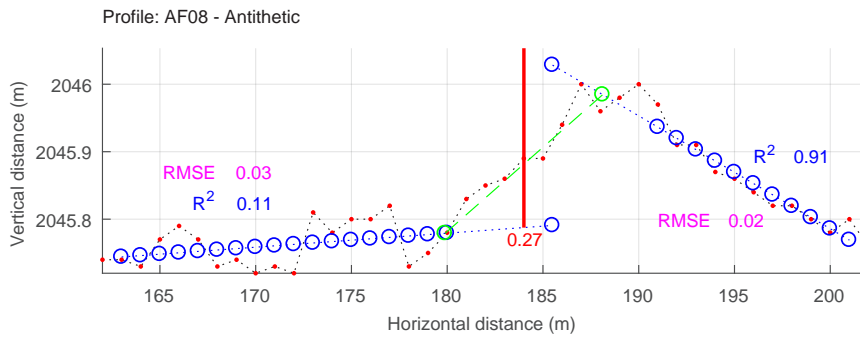
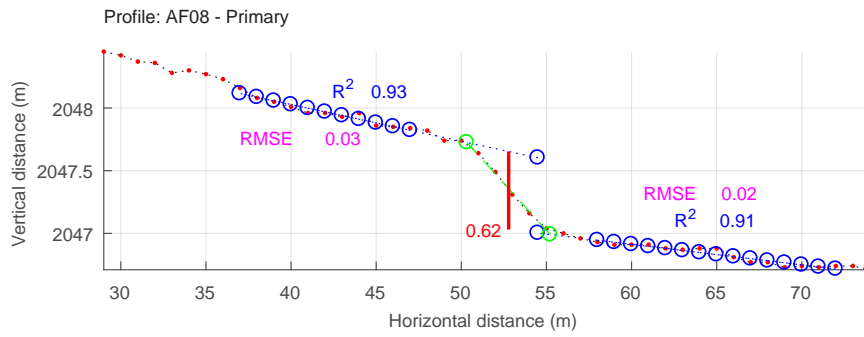
Elevation plot of AF06, including map of profile location and associate scarp and photograph.



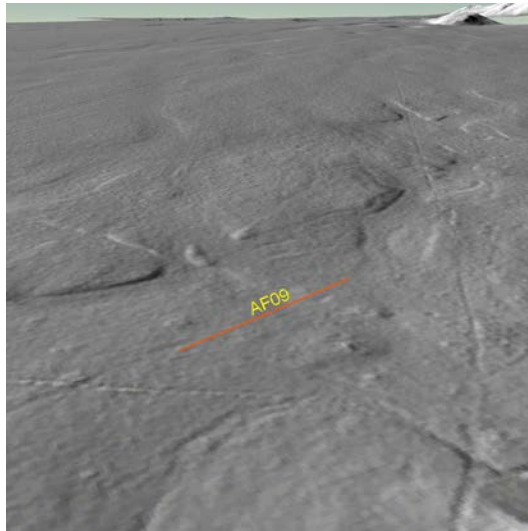
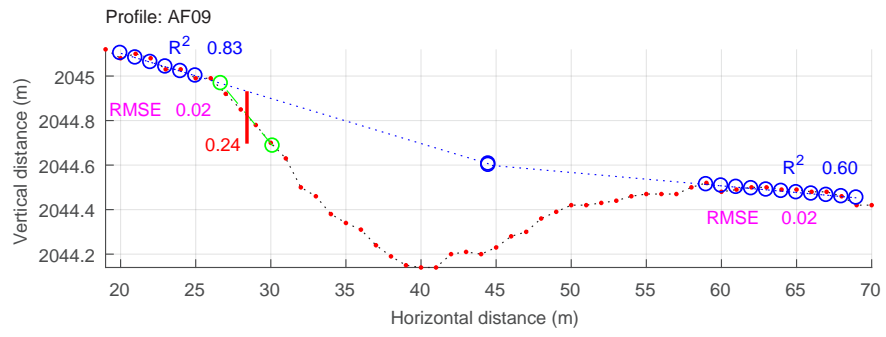
Elevation plots of AF07, including map of profile location and associate scarp and photograph.



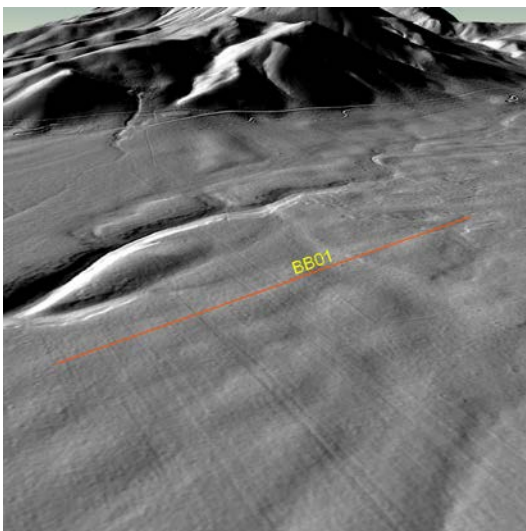
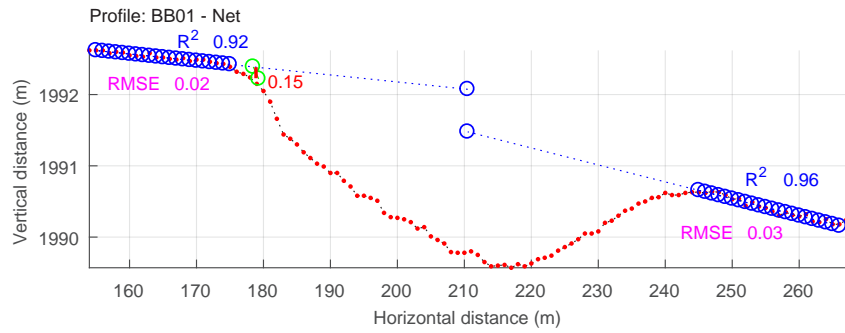
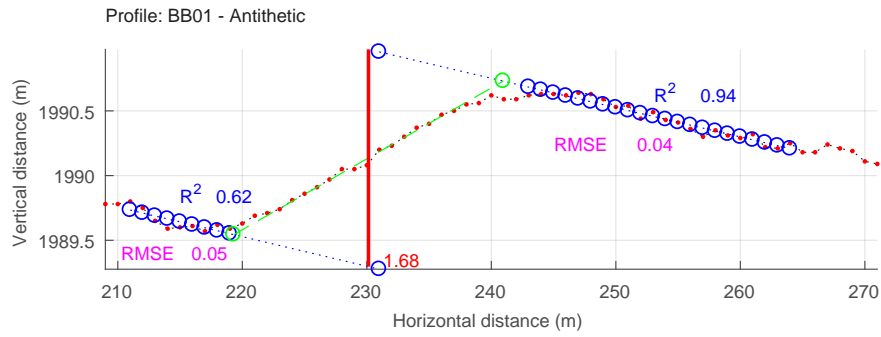
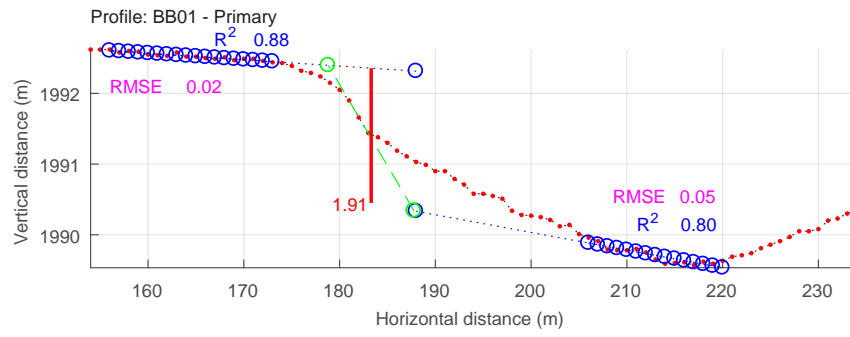
Elevation plots of AF08, including map of profile location and associate scarp and photograph.



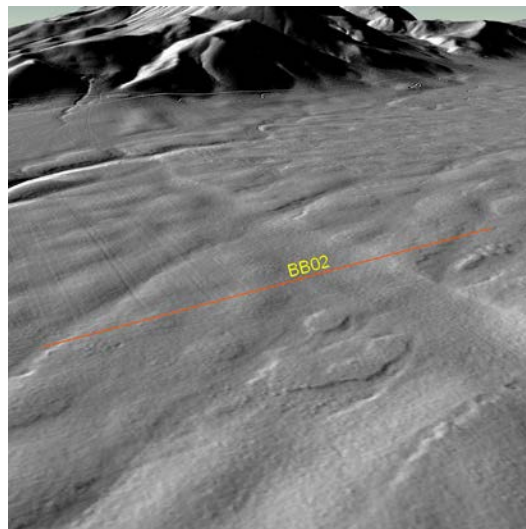
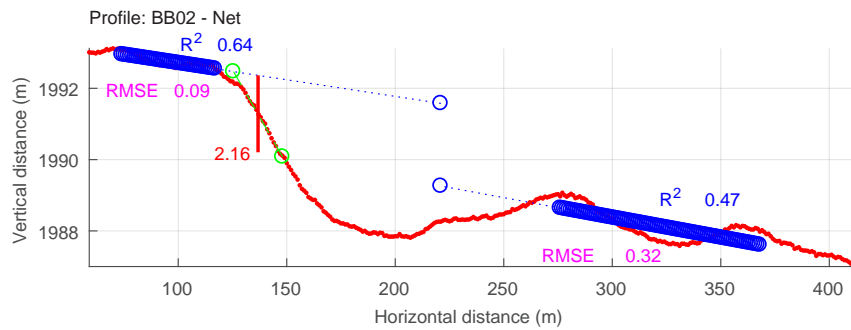
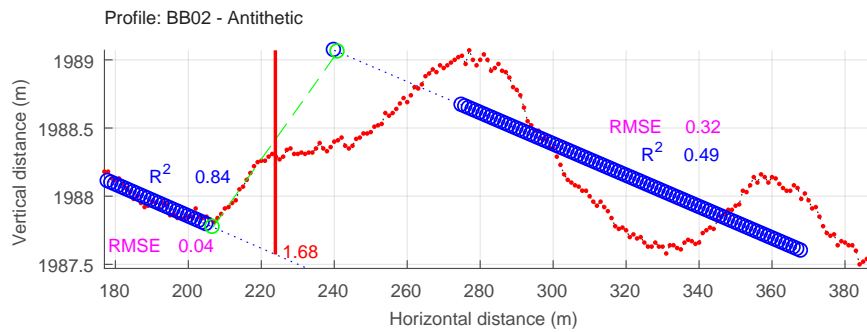
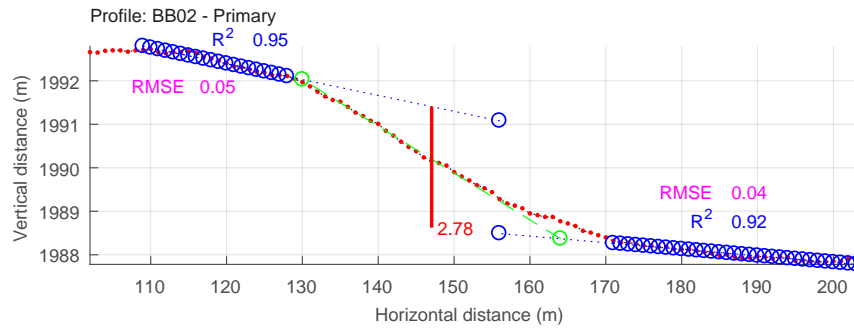
Elevation plot of AF09, including map of profile location and associate scarp.



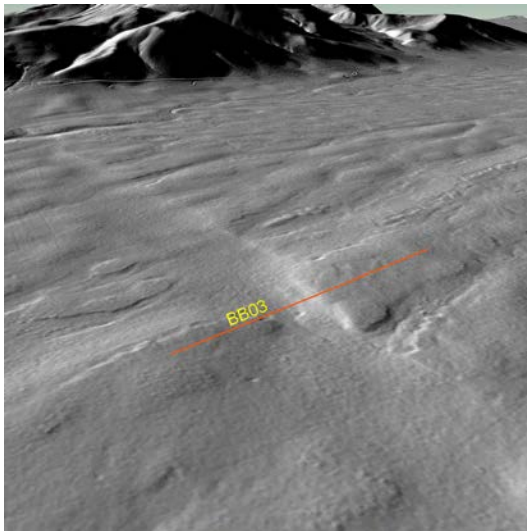
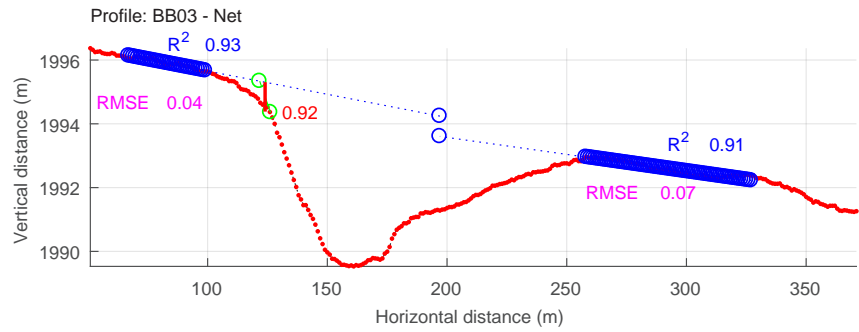
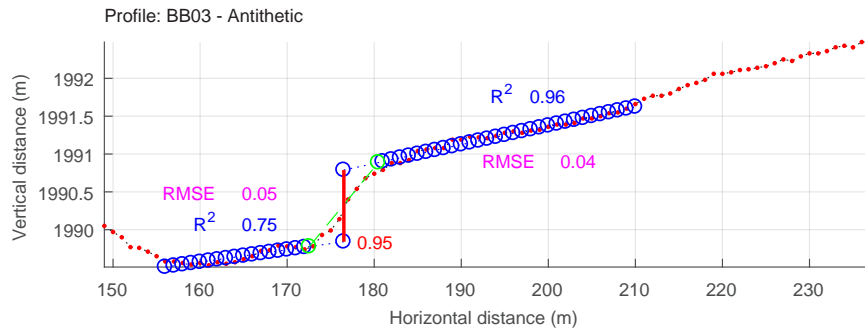
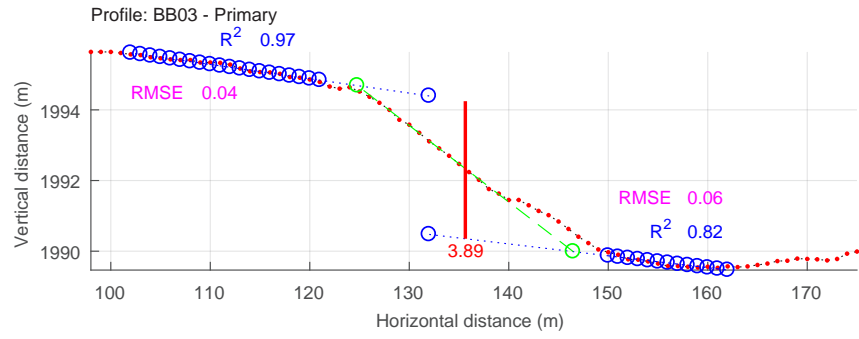
Elevation plots of BB01, including map of profile location and associate scarp and photograph.



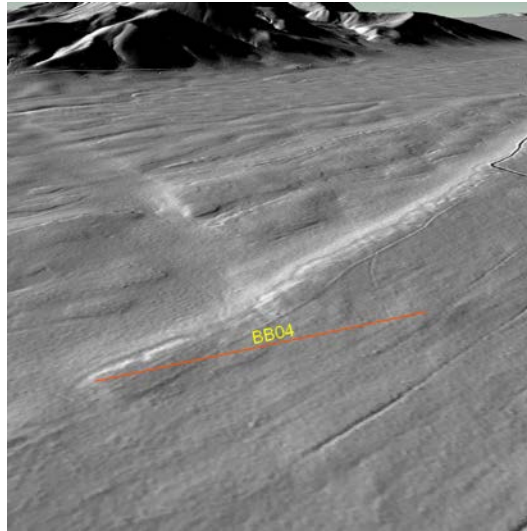
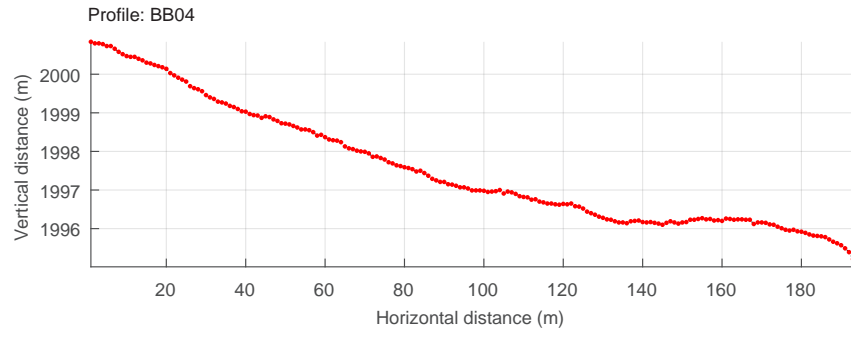
Elevation plots of BB02, including map of profile location and associate scarp.



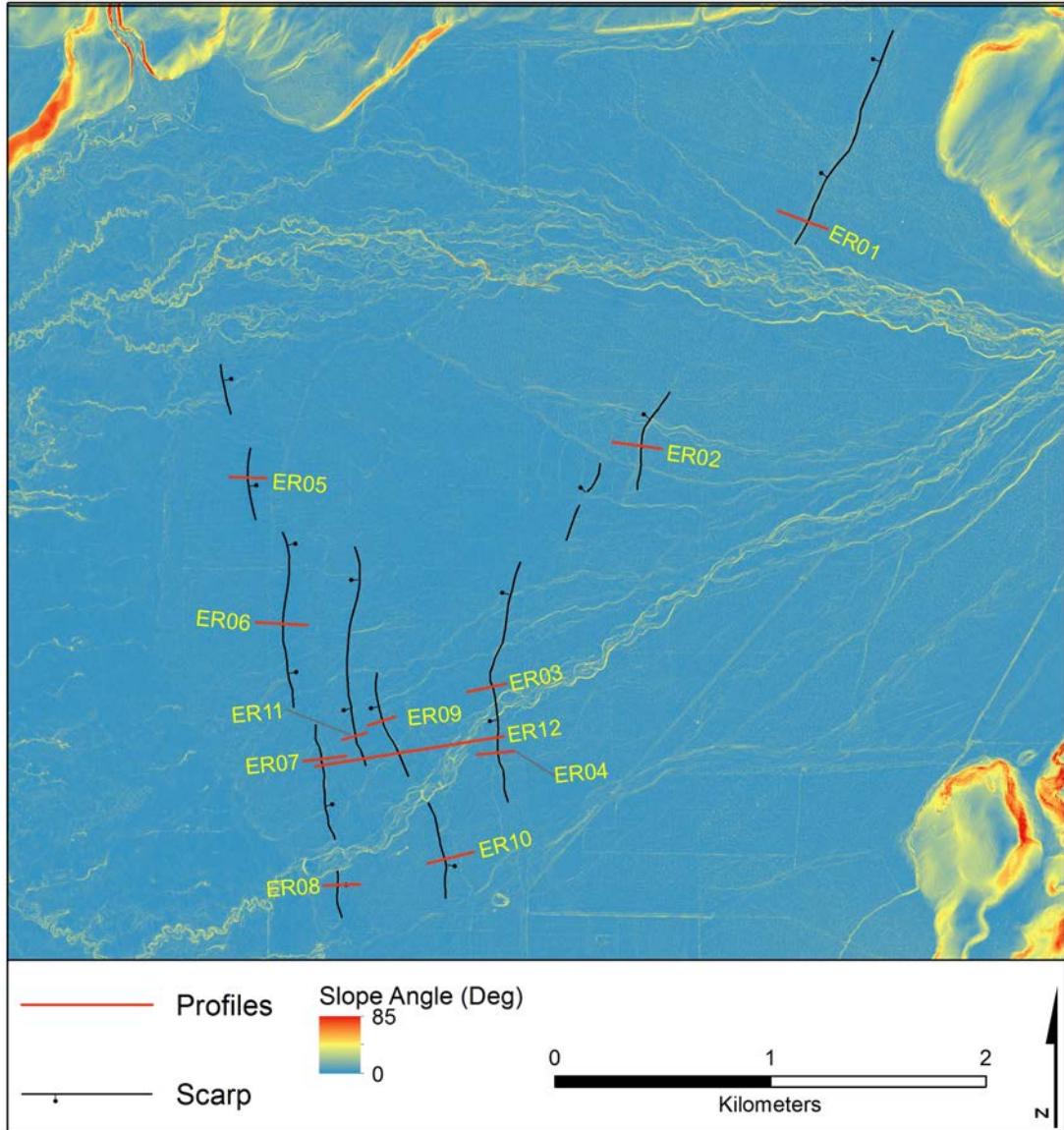
Elevation plots of BB03, including map of profile location and associate scarp and photograph.



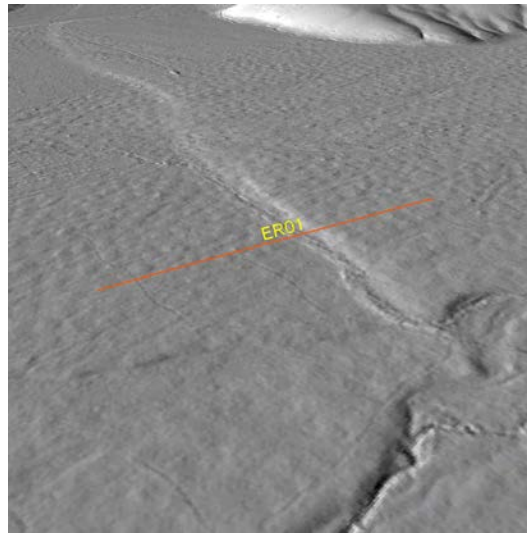
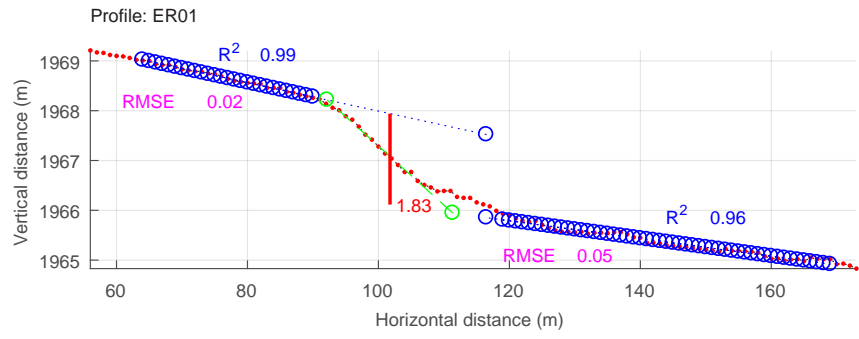
Elevation plot of BBO4, including map of profile location and associate scarp.



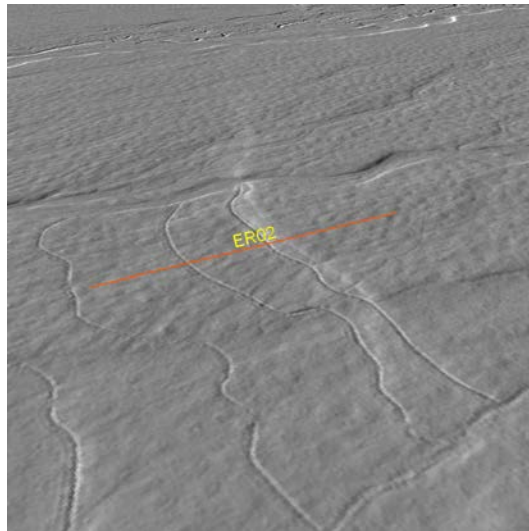
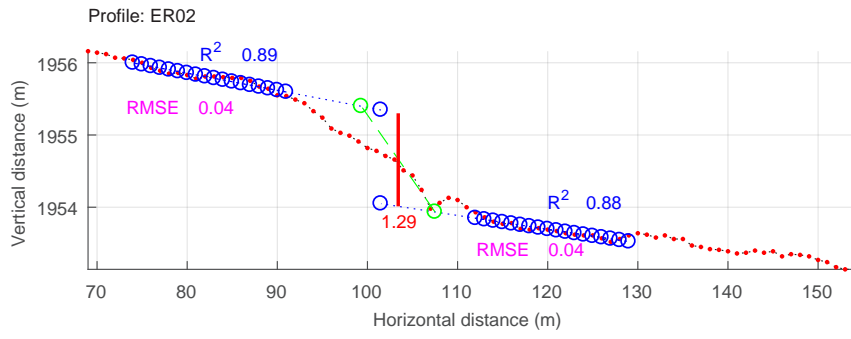
Map of profile locations at Flat Creek.



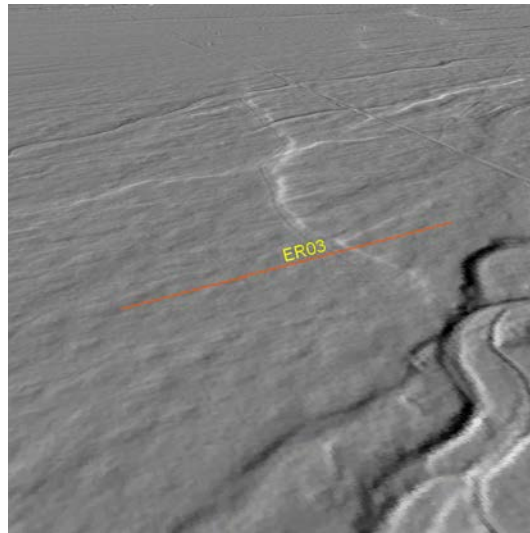
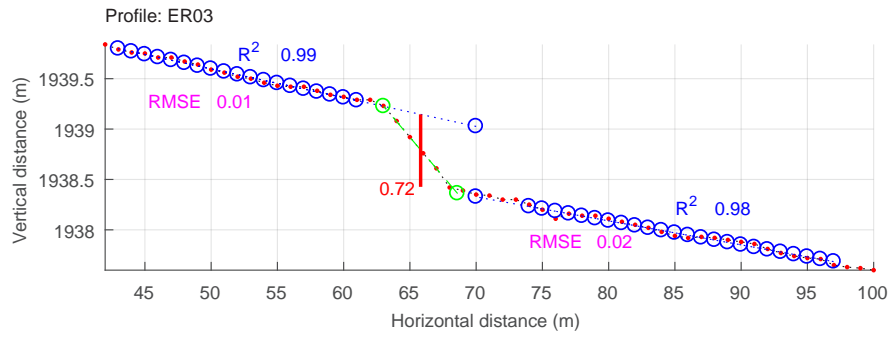
Elevation plot of ER01, including map of profile location and associate scarp and photograph.



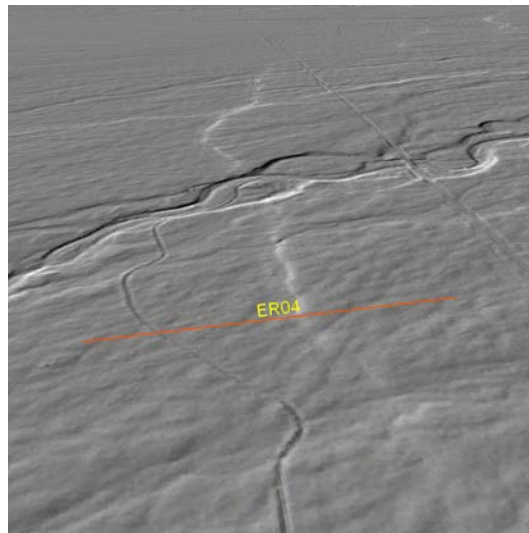
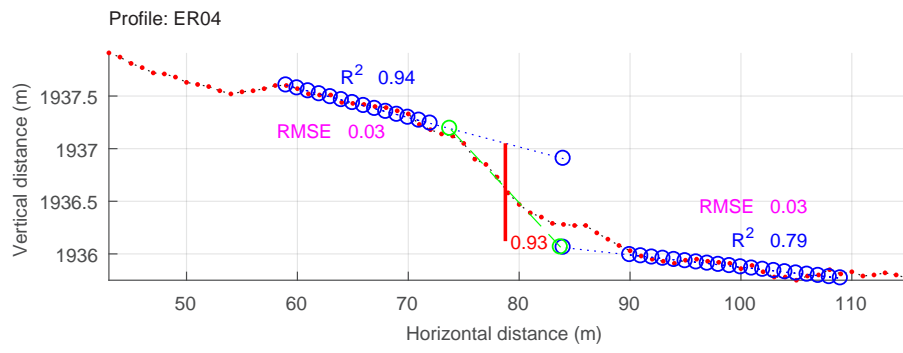
Elevation plot of ER02, including map of profile location and associate scarp.



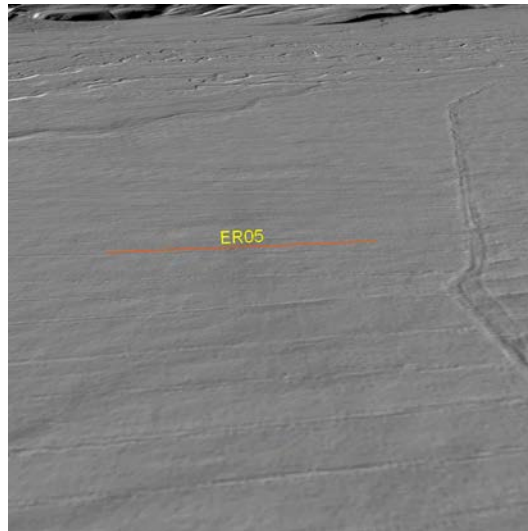
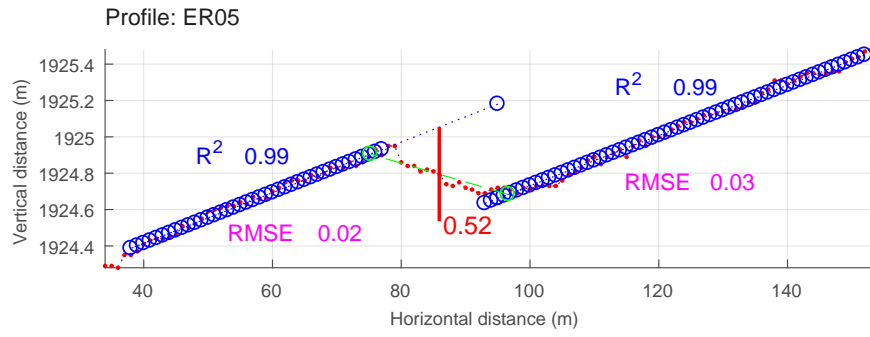
Elevation plot of ER03, including map of profile location and associate scarp.



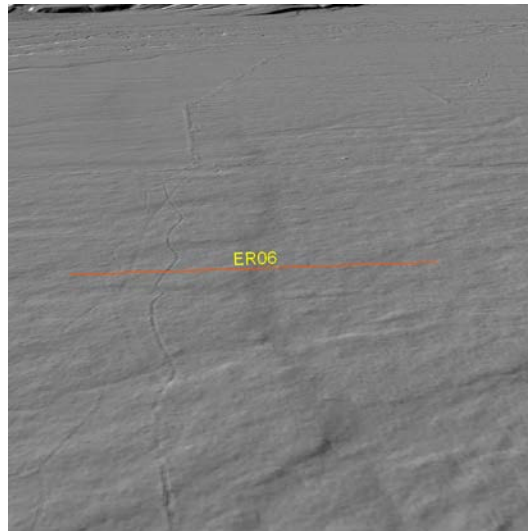
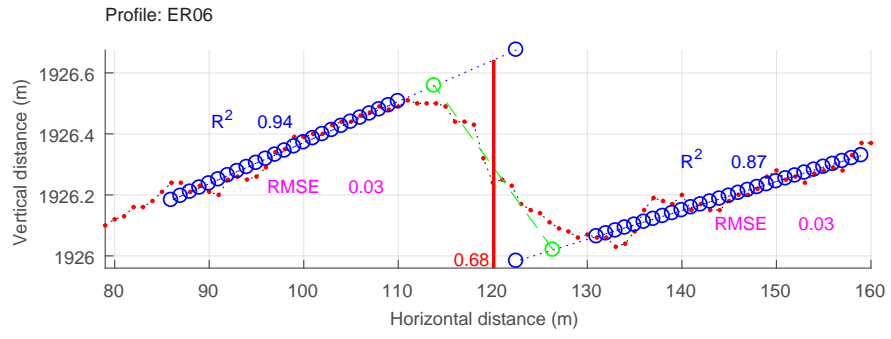
Elevation plot of ER04, including map of profile location and associate scarp.



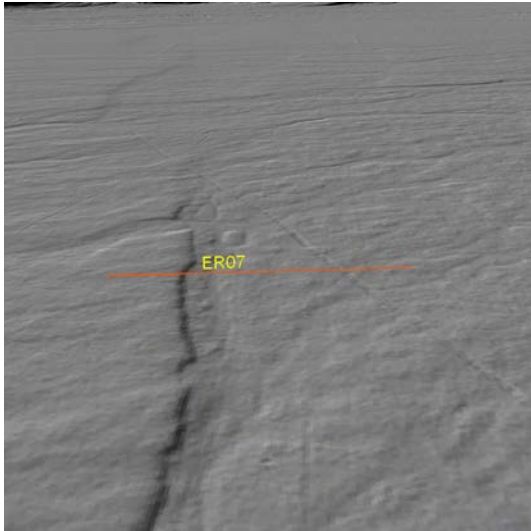
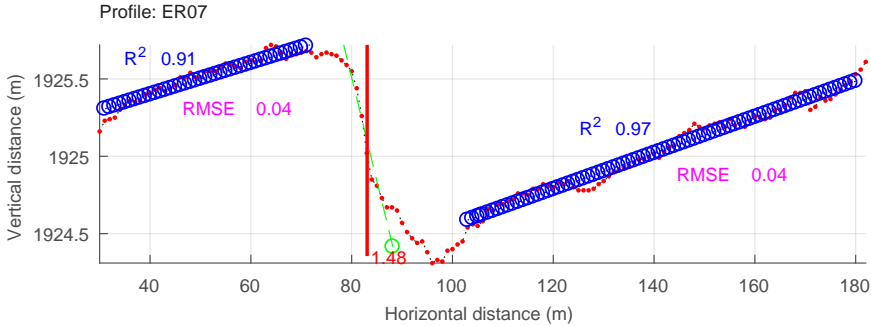
Elevation plot of ER05, including map of profile location and associate scarp.



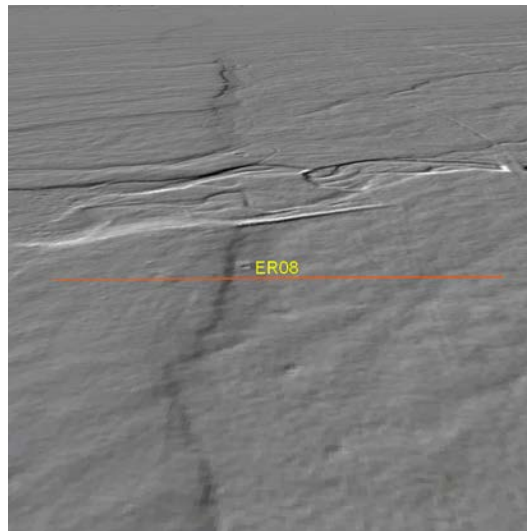
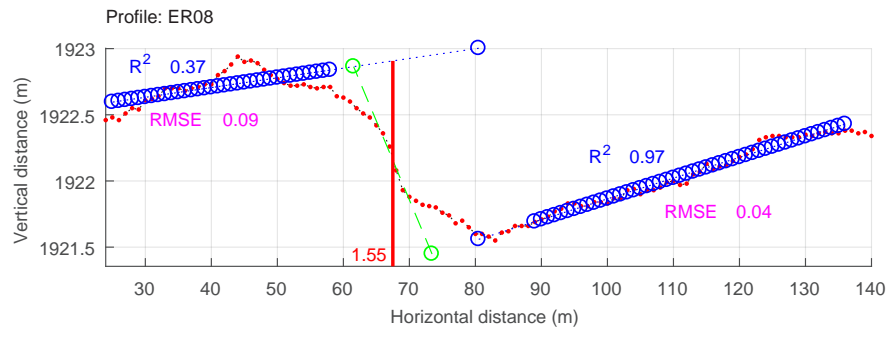
Elevation plot of ER06, including map of profile location and associate scarp.



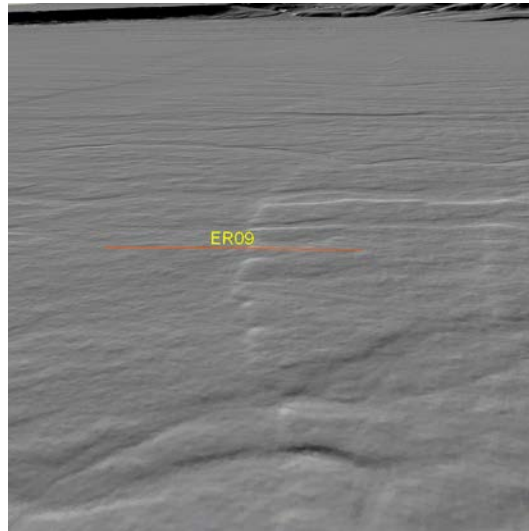
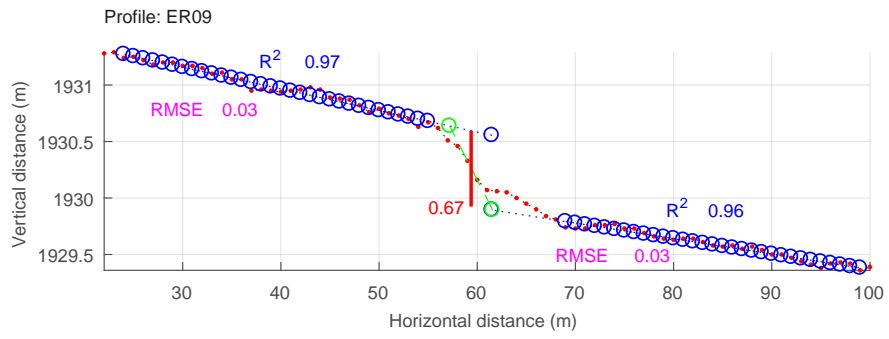
Elevation plot of ER07, including map of profile location and associate scarp and photograph.



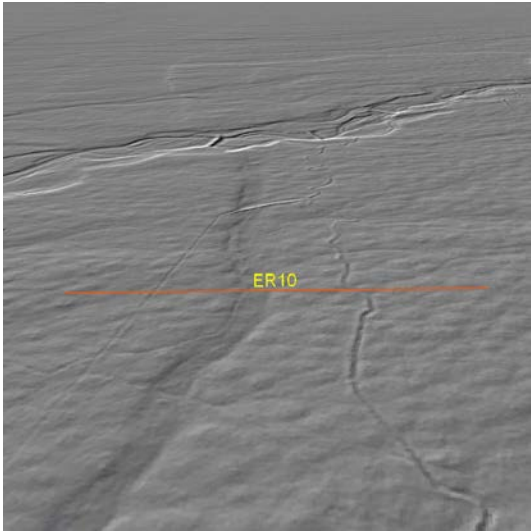
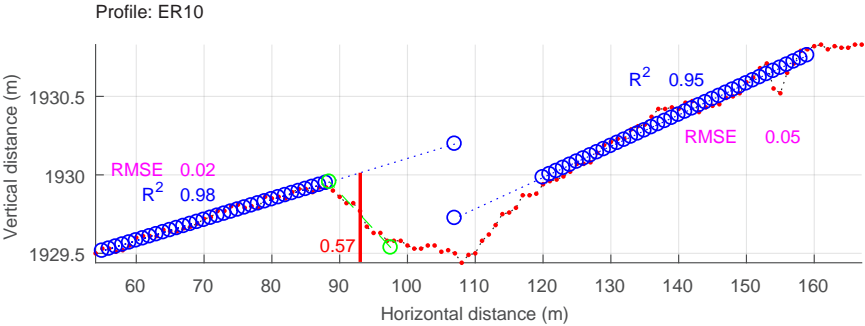
Elevation plot of ER08, including map of profile location and associate scarp.



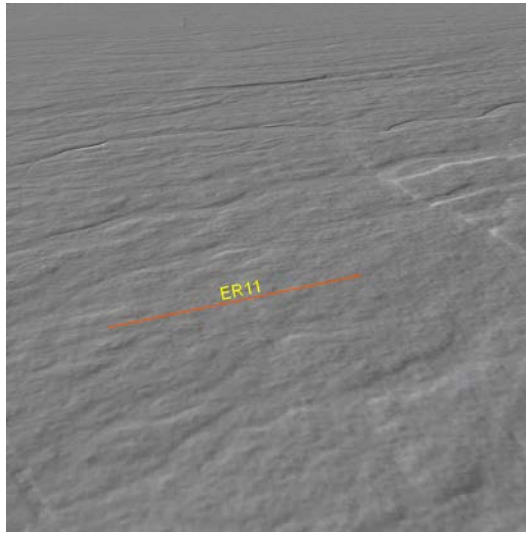
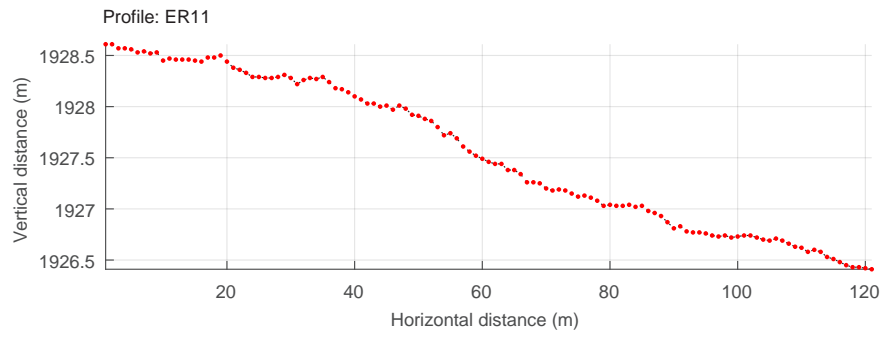
Elevation plot of ER09, including map of profile location and associate scarp and photograph.



Elevation plot of ER10, including map of profile location and associate scarp and photograph.



Elevation plot of ER11, including map of profile location and associate scarp.



Elevation plot of ER12, including map of profile location and associate scarp.

